Regulation of cardiac nitric oxide signaling by nuclear β-adrenergic and endothelin receptors*

George Vaniotis[a,c], Irina Glazkova[d,§], Clémence Merlen[a,c,§], Carter Smith[d], Louis R. Villeneuve[c], David Chatenet[e], Michel Therien[f], Alain Fournier[e], Artavazd Tadevosyan[b,c], Phan Trieu[d], Stanley Nattel[c,d], Terence E. Hébert[d] and Bruce G. Allen[a,b,c,d]

From the Departments of [a]Biochemistry and [b]Medicine, Université de Montréal, Montreal, Quebec H3T 1J4, Canada; [c]Montreal Heart Institute, Montréal, Québec, H1T 1C8, Canada; [d]Department of Pharmacology and Therapeutics, McGill University, Montréal, Québec, H3G 1Y6, Canada; [e]Laboratoire d'Études Moléculaires et Pharmacologiques des Peptides, Institut National de la Recherche Scientifique – Institut Armand-Frappier, Université du Québec, Laval, Quebec, H7V 1B7, Canada; and [f]Zamboni Chemistry Solutions, Department of Chemistry, McGill University, Montreal, Quebec, Canada

§ Both authors contributed equally to this work

To whom correspondence should be addressed:
Terence E. Hébert, Department of Pharmacology and Therapeutics, McGill University Faculty of Medicine, McIntyre Medical Sciences Building, 3655 Promenade Sir William Osler, Room 1303, Montréal, Québec, H3G 1Y6, Canada. Tel.: (514) 398-1398; Fax: (514) 398-6690; E-mail: terence.hebert@mcgill.ca
Bruce G. Allen, Department of Medicine, Montreal Heart Institute, Université de Montréal, 5000 Belanger St., Montréal, Québec, H1T 1C8, Canada. Tel.: (514) 376-3330 Ext. 3591; Fax: (514) 376-1355; E-mail: bruce.g.allen@umontreal.ca

Running head: Nuclear GPCRs regulate NO in cardiomyocytes

Abstract

At the cell surface, βARs and endothelin receptors can regulate nitric oxide (NO) production. β-adrenergic receptors (βARs) and type B endothelin receptors (ETB) are present in cardiac nuclear membranes and regulate transcription. The present study investigated the role of the NO pathway in the regulation of gene transcription by these nuclear G protein-coupled receptors. Nitric oxide production and transcription initiation were measured in nuclei isolated from adult rat heart. The cell-permeable fluorescent dye 4,5-diaminofluorescein diacetate (DAF2 DA) was used to provide a direct assessment of nitric oxide release. Both isoproterenol and endothelin increased NO production in isolated nuclei. Furthermore, a β_3AR-selective agonist, BRL 37344, increased NO synthesis whereas the β_1AR-selective agonist xamoterol did not. Isoproterenol increased, whereas ET-1 reduced, *de novo* transcription. The NO synthase inhibitor L-NAME prevented isoproterenol from increasing either NO production or *de novo* transcription. L-NAME also blocked ET-1-induced NO-production but did not alter the suppression of transcription initiation by ET-1. Inhibition of the cGMP-dependent protein kinase (PKG) using KT5823 also blocked the ability of isoproterenol to increase transcription initiation. Furthermore, immunoblotting revealed eNOS, but not nNOS, in isolated nuclei. Finally, caged, cell-permeable isoproterenol and endothelin-1 analogs were used to selectively activate intracellular β-adrenergic and endothelin receptors in intact adult cardiomyocytes. Intracellular release of caged ET-1 or isoproterenol analogs increased NO production in intact adult cardiomyocytes. Hence, activation of the NO synthase/guanylyl cyclase/PKG pathway is necessary for nuclear β_3ARs to increase *de novo* transcription. Furthermore, we have demonstrated the potential utility of caged receptor ligands in selectively modulating signaling via endogenous intracellular G protein-coupled receptors.

Keywords. β-adrenergic receptors, endothelin receptors, nuclear membranes, transcription, Nitric oxide, protein kinase G

1. Introduction

The G protein-coupled receptor (GPCR)[7] superfamily consists of a large group of seven transmembrane domain-containing receptors that signal via heterotrimeric G proteins. GPCRs modulate a wide range of downstream effectors and, as a result, regulate multiple cellular functions in cardiomyocytes. β-adrenergic receptors (βARs) and endothelin receptors (ETRs) are two such members of the GPCR superfamily, both of which are expressed in the myocardium. Recently, potential roles for these receptors when localized to intracellular compartments such as the nuclear membrane have been identified under both physiological and pathological conditions (reviewed in [1, 2]). We have shown that ETB, β_1AR and β_3AR are present on the nuclear membrane in adult cardiomyocytes [3, 4]. In addition, several of their downstream effectors have also been identified at the level of the nucleus or nuclear membrane [5, 6]. These receptors have been shown to bind ligand, couple to effectors, and regulate gene expression in isolated nuclei, with the βARs having a stimulatory effect on transcription initiation, whereas ETB activation is inhibitory [7]. The precise signaling pathways involved in regulation of transcriptional initiation by GPCRs in the nuclear membrane have not been clearly defined and require further study.

Nitric oxide (NO) is an important signaling molecule involved in many physiological processes. NO is produced from the amino acid L-arginine via the action of NO synthases (NOS, [8]. There are three NOS subtypes: endothelial (eNOS), neuronal (nNOS) and inducible (iNOS) [8]. All three NOS subtypes are expressed in cardiomyocytes and play roles in cardiac physiology and pathology [9, 10]. In fact, NO has been linked to a wide variety of effects in both the heart and vasculature, from regulation of vascular tone and myocardial contractility to calcium handling and apoptosis [8, 11]. Regulation of NOS activity is complex, involving several mechanisms mediated by calcium, protein kinases, and NO levels [12, 13]. The exact effect exerted by NO however, appears to depend on the NOS isoform being activated, as well as its subcellular localization and mode of action [11, 14]. NO exerts its effects via modulation of guanylyl cyclase activity leading to increases in cyclic guanosine 3',5'-monophosphate (cGMP)

levels and the subsequent activation of protein kinase G (PKG), but has also been shown to signal in a guanylyl cyclase-independent manner [15]. NO has also been implicated in the regulation of gene expression through the transcriptional regulator nuclear factor κB (NF-κB) [15, 16]. In addition, recent findings have also demonstrated that the PI3K/PKB pathway, which is activated by nuclear βARs [7], is capable of activating both eNOS and iNOS, leading to the stimulation of NO production [17, 18]. Moreover, iNOS upregulation in the nucleus appears to be linked to $G\alpha_i$, the protein kinase ERK1/2, and potentially eNOS as well [19-21]. Furthermore, a link has also been established between NO production and both ETA and ETB [22] as well as the βARs [10, 23] localized at the cell surface. Additionally recent evidence has also shown a role for NO in the nucleus, where it appears to modulate calcium homeostasis and is also potentially regulated by ET-1 [20, 24].

Given the involvement of NO in the regulation of cardiac function, and its established link with both the ETRs and βARs, we wished to ascertain whether the NO pathway was involved in the regulation of gene expression observed following stimulation of nuclear ETRs and βARs, and to identify which components of NO signaling might be implicated. Toward this end, we used a pharmacologic approach to study NO production in both isolated nuclei and intact cardiomyocytes following treatment with various agonists and inhibitors. Further, we demonstrate the potential utility of caged receptor ligands in selectively modulating nuclear signaling via GPCRs.

2. Materials and Methods

2.1. Materials

Triton X-100 (TX-100), leupeptin, PMSF and DNase I were from Roche Applied Science (Laval, Quebec). Isoproterenol, BRL 37344, CGP20712, ICI118551, SR59230A, 8-bromo-cGMP, Rp-8-Br-PET-cGMPS (Rp-8-Br) and KT5823 were from Tocris (Ellisville, MO). Endothelin-1 (ET-1) was from Peninsula Labs (Torrance, CA). Pertussis toxin (PTX), xamoterol, forskolin, alprenolol, EEDQ and L-NAME, were from Sigma-Aldrich (Mississauga, Ontario). Triciribine, diaminofluorescein-2 (DAF-2), and diaminofluorescein-2 diacetate (DAF-2 DA) were from Calbiochem. RNaseOut, dNTP Mix, First Strand buffer, and M-MLVRT were from Invitrogen. Primers, as well as SYBR Green and ROX were also from Invitrogen. RNA extraction kits were from Qiagen. DRAQ5 was from Enzo Life Sciences (Farmingdale, NY). nNOS- and eNOS-selective antibodies were from Cell Signaling Technology and BD Transduction Laboratories, respectively. Horseradish peroxide (HRP)-conjugated secondary antibodies were from Jackson ImmunoResearch Laboratories (West Grove, PA). Enhanced chemiluminescence (ECL) reagent Renaissance Plus was from Perkin Elmer Life Sciences (Woodbridge, Ontario). SDS-polyacrylamide gel electrophoresis (SDS-PAGE) reagents and nitrocellulose (0.22 μm) were from Bio-Rad Laboratories (Mississauga, Ontario). Bovine aortic endothelial cells (BAEC) were a generous gift from Dr. Martin Sirois (Montréal Heart Institute). Unless otherwise stated, all reagents were of analytical grade and were purchased from VWR Canlab (Ville Mont-Royal, Quebec) or Fisher Scientific (Mississauga, Ontario). [α^{32}P]UTP (specific activity 3000 Ci/mmol) and [^{125}I]CYP were from Perkin Elmer (Montreal, Quebec).

2.2. Synthesis of caged isoproterenol

Previous studies have shown that it is possible to create caged versions of isoproterenol [25]. We wanted to engineer a more hydrophobic version that would be more readily absorbed by cells before uncaging with UV light. The caged compounds were prepared by treatment of the

amine starting material, isoproterenol, with the corresponding 2-nitrobenzyl bromide in dimethylsulfoxide and potassium carbonate as shown in Figure 1. After purification by silica gel column chromatography, the desired amines were treated with HCl in dioxane to obtain the hydrochloride salt. To (-)-isoproterenol hydrochloride, (150 mg) in DMSO (1.8 mL), was added 2-bromomethyl-4-methoxy-1-nitrobenzene (149 mg) and potassium carbonate (169 mg). The mixture was stirred overnight, then diluted with dichloromethane, washed with water (2X), brine and dried over Na_2SO_4, filtered, and the solvent evaporated. Purification by silica gel chromatography yielded 81 mg (R)-4-[1-hydroxy-2-[isopropyl-(5-methoxy-2-nitrobenzyl)-amino]-ethyl]-benzene-1,2-diol which was dissolved in diethyl ether and treated with 4 M HCl in dioxane (0.16 mL) to form a precipitate which was stirred for 1 h, then filtered and air dried, affording the desired (R)-4-[1-hydroxy-2-[isopropyl-(5-methoxy-2-nitrobenzyl)-amino]-ethyl]-benzene-1,2-diol hydrochloride. This compound is referred to herein as ZCS-1-67.

2.3. Isolation of nuclei

Rat cardiac nuclei were isolated and the purity of the nuclear preperation was tested as described previously [3, 26]. Briefly, rat hearts were pulverized under liquid nitrogen, resuspended in cold PBS, and homogenized (Polytron, 8000 rpm; 2 × 10 s). All subsequent steps were carried out on ice or at 5 °C. Homogenates were centrifuged for 15 min at 500 ×g. The supernatants were diluted 1:1 with buffer A (10 mM K-HEPES pH 7.9, 1.5 mM $MgCl_2$, 10 mM KCl, 1 mM DTT, 25 μg/mL leupeptin, 0.2 mM Na_3VO_4), incubated 10 min on ice, and centrifuged for 15 min at 2000 ×g. The resulting supernatant was then discarded. The pellet was resuspended in buffer B (0.3 M K-HEPES pH 7.9, 1.5 M KCl, 0.03 M $MgCl_2$, 25 μg/mL leupeptin, 0.2 mM Na_3VO_4), incubated on ice for 20 min, and centrifuged for 15 min at 2000 ×g. The pellet, an enriched nuclear fraction, was resuspended in buffer C (20 mM Na-HEPES pH 7.9, 25% (v/v) glycerol, 0.42 M NaCl, 1.5 mM $MgCl_2$, 0.2 mM EDTA, 0.2 mM EGTA, 0.5 mM PMSF, 0.5 mM DTT, 25 μg/mL leupeptin, 0.2 mM Na_3VO_4) or 1× transcription buffer (50 mM Tris pH 7.9, 0.15 M KCl, 1 mM $MnCl_2$, 6 mM $MgCl_2$, 1 mM ATP, 2 mM DTT, 1 U/μL RNAse

inhibitor) and used fresh.

2.4. Measurement of NO production

Isolated nuclei were preincubated with the fluorescent dye DAF-2 (5 μg/mL) in a buffer containing 140 mM NaCl, 14 mM glucose, 4.7 mM KCl, 2.5 mM $CaCl_2$, 1.8 mM $MgSO_4$, 1.8 mM KH_2PO_4, and 0.1 mM L-arginine (final pH 7.4) for 30 min at 37 °C. Nuclei were washed twice in standard buffer to remove any unbound dye and then resuspended in our nuclear isolation buffer C. The inhibitors used were L-NAME (1 mM, 30 min at 37 °C), PTX (5 μg/mL, 2 h at 37 °C), KT5823 (1 μM, 30 min at 37 °C), Rp-8-Br-PET-cGMPS (1 μM, 1 h at 37 °C) and triciribine (1 μM, 30 min at 37 °C). Pre-treatment with subtype-selective βAR antagonists CGP20712 (5 nM, 30 min at 37 °C), ICI 118,551 (10 nM, 30 min at 37 °C) and SR59230A (1 μM, 30 min at 37 °C) was also performed in certain experiments. Nuclei were then treated with either isoproterenol (1 μM), ET-1 (10 nM), BRL 37344 (1 μM), xamoterol (1 μM), forskolin (100 nM) or vehicle for 30 min at 37 °C. DAF fluorescence, indicating NO production, was measured using a microplate reader at wavelengths of 485 nm (excitation) and 510 nm (emission) and expressed as arbitrary fluorescence units (AU).

2.5. Transcription initiation

Measurements of transcription initiation were performed as previously described [4]. Briefly, 10 μL of freshly isolated nuclei (resuspended in 1× transcription buffer) were incubated at 30 °C for 30 min in a final volume of 20 μL containing agonist/antagonist and 10 μCi [α^{32}P]UTP (3000 Ci/mmol) in the absence of CTP and GTP to prevent chain elongation. Following termination of reactions by digestion with DNase I, nuclei were lysed with 10 mM Tris-HCl pH 8.0, 10 mM EDTA and 1% SDS. Duplicate 5 μL aliquots were transferred onto Whatman GF/C glass fibre filters, washed twice with 5% TCA containing 20 mM sodium pyrophosphate, and air-dried. Incorporation of [^{32}P] was determined by liquid scintillation counting. DNA concentrations were determined by spectrophotometry. [^{32}P] incorporation was

expressed as dpm/ng DNA. Where indicated, isolated nuclei were pre-treated at 37 °C with 1 mM L-NAME, 1 μM KT5823, 1 μM Rp-8-Br, 100 μM cGMP or vehicle for 30 min.

2.6. Radioligand binding assays

Membranes prepared from naive HEK 293 cells and from a stable HEK 293 cell line expressing the β_2AR and preincubated with 100 μM EEDQ or vehicle for 2 h at 37 °C. Briefly, cells were washed twice with cold PBS and then 10 mL of lysis buffer (5 mM Tris-HCl pH 7.4, 2 mM EDTA, with protease inhibitor cocktail) was added to each flask. Cells were disrupted using a Polytron (2 × 10 s) on ice, and then centrifuged for 5 min at 1000 rpm and 4 °C. The lysate was centrifuged at 16000 rpm for 20 min at 4 °C and the pellet resuspended in 1 mL of binding buffer (75 mM Tris-HCl pH 7.4, 2 mM EDTA, 12.5 mM $MgCl_2$). Membranes from whole rat heart were prepared as previously described [27]. Briefly, hearts were pulverized under liquid nitrogen then homogenized by polytron in 15 mL of ice cold lysis buffer (5 mM Tris-HCl, pH 7.4, 2 mM EDTA, plus protease inhibitor cocktail). The resulting homogenate was centrifuged at 500 × g for 15 min at 4 °C. The supernatant was centrifuged at 45000 ×g for 15 min, and the pellet resuspended in binding buffer. [^{125}I]CYP (50 μL, 400,000 cpm) was added to 10 μL of membranes in a total volume of 0.5 mL, in triplicate, for each condition. Alprenolol (10 μM) was used to measure non-specific binding. In some cases, membranes were treated with ISO (1 μM), caged or uncaged ZCS-1-67 (1 and 5 μM) were used to compete with specific CYP binding. Membranes were incubated at room temperature for 90 min and subsequently captured and washed using a Brandel cell harvester. [^{125}I]CYP binding was quantified using a γ-counter.

2.7. EEDQ treatment

Calcium-tolerant cardiac ventricular cardiomyocytes were isolated from adult male Sprague-Dawley rats by Langendorff perfusion as previously described [28]. Freshly isolated cardiomyocytes were treated with either 100 μM EEDQ or vehicle (2 h, 37 °C) to irreversibly alkylate β-adrenergic receptors present at the cell surface, followed by treatment with either 1

μM isoproterenol or vehicle (30 min, 30 °C).

2.8. Quantitative real-time PCR

RNA was isolated from either purified nuclei or isolated myocytes using the Qiagen RNA extraction kit. To prepare cDNA, 1 μg of RNA was mixed with 100 ng of random primers and 1 μL of 10 mM dNTPs in a final volume of 10 μL, heated to 65 °C for 5 min, and then immediately quick chilled on ice. Next, 4 μL of 5× first strand buffer, 2 μL of 0.1 M DTT and 1 μL of RNAse Out were added and the reactions were then incubated for 2 min at 37 °C. Following addition of 1 μL of M-MLVRT (200 units), reactions were mixed, centrifuged and then incubated for 10 min at 25 °C, then at 37 °C for 50 min, and finally at 70 °C for 15 min. qPCR reactions, containing 12.5 μL of SyBR Green PCR master mix, 0.03 μL ROX dye (an internal fluorescence standard), 2.5 μL of primers, and 10 μL of cDNA were for 1 cycle of 10 min at 95 °C, then 40 cycles of (30 s at 95 °C, followed by 1 min at 60 °C and 1 min at 72 °C) using a Stratagene Mx3000P system. Samples were assayed in duplicate and normalized to β-actin expression. Primers used for real-time qPCR are shown in Table 1. The selectivity of the primers for a single product was validated by dissociation curve analysis.

2.9. Measurement of NO production in intact cells

Left ventricular cardiomyocytes were isolated from adult male rats as described previously [28] and plated on laminin-coated glass-bottomed culture dishes for 1 h at 37 °C (95% O_2, 5% CO_2) and 30 min at 4 °C. Cardiomyocytes were then incubated with DAF-2 DA (10 μM) in 20 mM HEPES pH 7.4, 134 mM NaCl, 6 mM KCl, 10 mM glucose, 2 mM $CaCl_2$, 1 mM $MgCl_2$ and 1% BSA (buffer D) for 30 min at room temperature and in the absence or presence of a photolabile caged isoproterenol (ZCS-1-67, 30 μM) or a photolabile caged ET-1 analog ([Trp-ODMNB^{21}]-ET-1, 1.5 μM) [29] and either the NO synthase inhibitor L-NAME (1 mM) or vehicle, as indicated. Cardiomyocytes were then washed three times with buffer D and a cell-permeable fluorescent DNA dye, DRAQ5 (1 μM), was added and L-NAME was re-added where

indicated. Fluorescence imaging was performed using a Zeiss LSM 7 Duo microscope (combining LSM 710 and Zeiss Live systems) with a 63x/1.4 oil Plan-Apochromat objective. DAF-2 DA was excited with a 488 nm/100 mW diode (2-3% laser intensity) and fluorescence emitted between 495 nm and 550 nm was collected. Cells were scanned approximately every 10 s. Pixel size was set at 0.264 μm and the pinhole at 2 Airy units. To visualize the nucleus, DRAQ5 was excited with a 635 nm/50 mW diode and fluorescence emitted at >655 nm was collected. DAF-2 DA and DRAQ5 were excited and fluorescence collected simultaneously using 2 different Zeiss Live detectors. Images were acquired over a total period of 9 min (60 frames). After acquiring 13 frames (114 s) to establish a baseline, cET-1 or ZCS-1-67 was photolysed by administering a 4 s pulse of UV light using a 405 nm/30 mW diode (100% laser intensity). DRAQ5 emissions were used to focus the UV laser into a 60 μm^2 rectangular region overlapping the nucleus. The microscope stage (Zeiss Observer Z1) was equipped with a BC 405/561 dichroic mirror that allowed simultaneous photolysis of ZCS-1-67 or caged ET-1 (LSM 710 405 nm laser) and image acquisition (Zeiss Live). Cardiomyocytes were maintained at 35-36 °C, using a stage incubator and objective heater, for the duration of image acquisition.

2.10. EPAC Assays for cAMP detection

HEK 293 cells were plated onto 6-well plates at least 24 h prior to transfection. The cells were transfected with 3 μg of EPAC construct [30] and 1 μg of FLAG-tagged β_2AR using 5 μL of Lipofectamine 2000. 72 h post transfection, the cells were washed twice with PBS and resuspended in 500 μl of PBS. Cell suspensions (80 μL) were distributed in 96-well Opti-plates and left to incubate for 2 h at room temperature. Fluorescence was then measured using a Synergy2 (Biotek) microplate reader. Immediately after reading the fluorescence, the cells were incubated with coelenterazine h (final well concentration 50 μM) and total luminescence and BRET ratios were collected for 5 min. The average of these BRET ratios represents basal BRET of the cells. ZCS-1-67 was exposed to 15 minutes of UV light (black-ray long wave, model B100AP lamp, Thermo-Fisher) 3.0 cm above the plate to uncage compounds prior to being

added to the assay plates. The cells were then stimulated by the addition of 10 μL of 100 μM isoproterenol prepared in 100 μM of ascorbic acid (final isoproterenol concentration 10 μM) or with 10 μl of 100 μM ascorbic acid (vehicle) and BRET ratios were read for 30 min. Upon completion of the assay, the final five BRET readings were averaged and taken to represent the final average BRET. The net BRET for agonist or vehicle treatment was calculated by subtracting basal BRET from the final average BRET. The ΔBRET for each transfection was then calculated by subtracting the net BRET of agonist from respective net BRET of vehicle.

2.11. Immunoblotting

SDS-PAGE and immunoblotting were performed as previously described [31]; however, nitrocellulose membranes were employed in the present studies.

2.12. Statistical analysis

Data are presented as the mean ± the standard error of the mean (S.E.M.). The significance of differences between groups was determined using one-way ANOVA followed by Tukey's multiple comparison tests (Prism 4.0cx, GraphPad Software). Differences were considered significant when $p < 0.05$.

3. Results

3.1. Measurement of NO production

The link between plasma membrane GPCR signaling and nitric oxide (NO) production has been well characterized for both the ETB [24, 32] and the βARs, including the β_3AR [8, 10]. Hence, given the presence of these receptors on the nuclear membrane, the recapitulation of cell surface signaling pathways in the nucleus (reviewed in [1, 2]) and the demonstrated effects of certain nuclear prostaglandin E2, bradykinin, lysophosphatidic acid type-1 receptors on iNOS and eNOS expression in non-cardiac cells [18-20, 33, 34], we sought to determine if either βARs or ETB also regulated NO production in cardiac nuclei. We first ascertained whether treatment of isolated rat heart nuclei with either isoproterenol or ET-1 resulted in a change in NO levels. Isolated rat heart nuclei were preincubated with the fluorescent dye DAF-2 and then treated with isoproterenol (ISO, 1 μM), ET-1 (10 nM) or vehicle, for 5, 10, 15, and 30 min. An increase in NO production could be detected as early as 5 min after treatment with either agonist, with a maximal response detectable at 30 min (Supplemental Figure 1). Hence, treatment was for 30 min in all subsequent experiments. Given that we observed a time-dependent increase in NO production following agonist treatment, we next wanted to determine if we could block this increase with the non-selective NOS inhibitor N-nitro-L-arginine methyl ester (L-NAME). Toward this end, isolated nuclei were again preincubated with the fluorescent dye DAF-2 and then incubated for 30 min with or without L-NAME (1 mM) before being treated with either ISO (1 μM, 30 min) or ET-1 (10 nM, 30 min, Figure 2A). Again, NO release increased following agonist treatment; however, pre-treatment of nuclei with L-NAME blocked this increase in both ISO and ET-1 treated nuclei. Immunoblot experiments using antibodies against the two constitutive NOS isoforms revealed that it is likely that eNOS is responsible for this effect, as eNOS immunoreactivity was detected in enriched nuclear preparations whereas nNOS was not (Supplemental Figure 2). Pre-treatment of isolated nuclei with two inhibitors of PKG, KT5823 or Rp-8-Br, did not alter the ability of ET-1 or ISO to increase NO release (Supplemental Figure 3).

However, treatment with either inhibitor alone resulted in an increase in NO production, indicating that PKG may inhibit NOS activity. Negative-feedback regulation of NOS activity by PKG has been observed previously in intact vascular endothelial cells [35, 36]. These results clearly demonstrate that both ETB and βARs can increase NOS activity in isolated cardiac nuclei, likely through activation of eNOS.

Given that two βAR subtypes, β_1AR and the β_3AR, were shown to be present at the level of the nuclear membrane [4], we next sought to determine which of these two βAR subtypes was responsible for the increase in NO production following ISO treatment. Thus, isolated nuclei preincubated with DAF-2 were treated with a β_1AR specific agonist, xamoterol, a β_3AR specific agonist, BRL37344, or forskolin, which can directly activate adenylyl cyclase (AC), bypassing the receptor (Figure 2B). Interestingly, the β_3AR-specific agonist had an effect similar to ISO, whereas xamoterol and forskolin had no appreciable effect on DAF-2 fluorescence. This was further confirmed with specific antagonists against all three βAR subtypes (Figure 2C). As expected, the β_3AR antagonist SR59230A was able to inhibit the increase in NO production produced by ISO while the β_1AR antagonist CGP20712 had no significant effect. Interestingly, the specific β_2AR antagonist ICI 118,551 also inhibited the ISO stimulated increase indicating that there may be differences in receptor selectivity between the nucleus and plasma membrane. We previously showed that ligand selectivity was altered when multiple βAR subtypes were co-expressed in the same cells [37]. Further study would be required to more carefully examine pharmacological differences between receptors on the nucleus versus the plasma membrane. Taken together, our data indicates that ISO regulates NOS activity via β_3AR whereas the β_1AR-mediated AC/cAMP pathway is not directly involved in isolated cardiac nuclei.

We next wished to determine which heterotrimeric G protein mediated the effects of β_3AR stimulation upon NOS activity in the nuclear membrane. Given that the AC/cAMP pathway did not seem to play a role, and that both the nuclear β_3AR [4] and ETB [38] can activate Gαi, we used pertussis toxin (PTX) to block Gαi activation. Of note is the fact that we have already shown that PTX inhibits ISO-stimulated increases in transcription initiation by β_3AR,

demonstrating the interaction between the receptor and Gαi [4]. Following preincubation with DAF-2, we pre-treated isolated nuclei with PTX (5 μg/mL, 2 h) and then treated with either ISO or ET-1. Interestingly, PTX treatment alone was able to increase the basal level of NO production in isolated nuclei, and to such an extent that further treatment with either agonist had no further appreciable effect (Figure 3A). This suggests that, in the absence of receptor stimulation, basal Gαi tone integrating inputs from several nuclear Gi-coupled GPCRs may play a role in modulating NOS activation and maintaining the basal levels of NO release. PTX prevents Gαi from functionally coupling with these different receptors might explain why no further increase is seen in the agonist treated samples, as both stimulatory and inhibitory inputs would both be lost. Identifying other putative Gαi-coupled receptors at the level of the nucleus leading to additional regulation of NO production would be an interesting avenue for future investigation. Alternatively, interactions with other G proteins, potentially Gαq in the case of ETB, might also be involved in regulating NOS activity.

Given the established link between PKB and ETRs [39] and nuclear βARs [7], as well as the well-characterized regulation of NOS activation by PKB [17, 21], we next examined the effect of PKB inhibition on NO production in isolated cardiac nuclei. Toward this end, isolated nuclei were loaded with DAF-2, then pre-treated with the PKB inhibitor triciribine (1 μM, 30 min), and finally treated with either ISO or ET-1. While treatment with either agonist lead to an increase in NO production, concomitant treatment with triciribine actually potentiated this effect, for both agonists, although to a lesser extent for ET-1 (Figure 3B). Treatment with triciribine alone, however, had no effect on basal NO production. Hence, PKB inhibition can lead to an increase in NO production, but only when the receptors are activated: basal activity was unaffected. The exact mechanism responsible for the potentiation remains to be elucidated. However, this might be explained in part by the mode of action of triciribine, which inhibits PKB activation, but whose exact molecular target is unknown. This would also leave the upstream effectors of PKB active; hence if they are activating other kinases as well they may be compensating for the lack of PKB activity. In addition while PKB is known to activate NO

production in the cytoplasm, it is entirely possible that a different signaling mechanism exists at the level of the nucleus. We have previously shown that the βARs activate the PI3K/PKB signaling pathway in isolated nuclei and that treatment with triciribine profoundly alters the modulation of transcription initiation, switching ISO from an agonist to an inverse agonist [7].

3.2. Transcription initiation

We next determined if NOS activation played a role in the previously described effects of ISO and ET-1 on transcription initiation in isolated cardiac nuclei [4, 7]. Thus, isolated nuclei were treated with either ISO (1 μM) or ET-1 (10 nM) in the presence or absence of L-NAME (1 mM). Transcription was assessed by measuring [α^{32}P]UTP incorporation. As previously reported, ISO increased *de novo* transcription (Figure 4A). L-NAME inhibited both the basal and ISO-induced increase in *de novo* transcription. ET-1, in the absence or presence of L-NAME, reduced [^{32}P] UTP incorporation to a level comparable to that induced by L-NAME alone. Hence, although ISO and ET-1 both increased NO release in isolated nuclei, they induced opposite effects on the initiation of global transcription, indicating there exists additional complexity in the organization of the two pathways.

NO exerts its effects by activation of soluble guanylyl cyclase and, possibly, by S-nitrosylation of cysteine residues in target proteins (see [11]). Hence cGMP-mediated activation of PKG may represent a means whereby activation of either β_3AR or ETB is transduced into changes in promoter activity. To further investigate this possibility, we examined the effect of PKG inhibition on transcription. Isolated nuclei were treated with either ISO (1 μM), ET-1 (10 nM) or cGMP (100 μM) in the presence or absence of 1 μM KT5823 or 1 μM Rp-8-Br, PKG inhibitors, and transcription initiation was assessed as [α^{32}P]UTP incorporation (Figure 4B). As with L-NAME, KT5823 exhibited an inhibitory effect on *de novo* transcription in the absence of agonist, and was also able to block the stimulatory effect of ISO. KT5823 alone reduced the basal level of [^{32}P]UTP incorporation to levels comparable to those induced by ET-1. While inhibition of PKG resulted in an increase in NO production, it is perhaps not unexpected to see a

decrease in transcription as PKG is likely involved in a feedback inhibition loop (discussed above), and thus the increased NO production is likely an attempt to compensate for the inhibition of PKG activity. Unlike KT5823, Rp-8-Br had no significant effect on the basal level of transcription likely due to the fact that it acts as a competitive inhibitor of cGMP and hence has no effect on the pool of already activated PKG. Rp-8-Br did however still inhibit the ISO stimulated increase. Furthermore, in the presence of ET-1 neither of these agents had any additional significant inhibitory effect upon transcription initiation. The inability of ET-1 to increase *de novo* transcription may reflect the fact that ISO increases the abundance of 18S ribosomal RNA (rRNA) [7] whereas ET-1 does not (Figure 4C) and rRNA accounts for approximately 90% of the total RNA pool. Microarray analysis has revealed that ET-1 and ISO regulate transcription of distinct, but overlapping, populations of genes in isolated cardiac nuclei (GV, TEH and BGA, in preparation). Treatment with cGMP had no significant effect on the basal level of transcription, though a slight inhibition was observed. Taken together, these results raise the possibility that PKG is involved in mediating the effects of nuclear βAR activation upon transcription, though further study is required to determine its exact role. ETB activation, although increasing NO production, may act to suppress the stimulatory effects of the NOS-GC-PKG pathway upon 18S RNA expression through the activation of additional signaling pathways. Alternatively, β_3ARs may activate one or more additional signaling pathways required for the initiation of 18S RNA transcription.

3.3. Nuclear GPCRs in intact cardiomyocytes

We next extended our findings into the context of the intact cardiomyocyte as isolated cardiac nuclei are derived from a heterogenous cell population and, in addition, would lack regulatory elements normally recruited from the cytosol. We have previously shown that the treatment of isolated nuclei with ISO increases the levels of 18S rRNA [7]. Hence, we first ascertained that we could reproduce the changes in 18S rRNA following ISO treatment in the intact cardiomyocyte. To ensure that the changes in 18S rRNA were in fact due to the specific

action of ISO upon nuclear βARs, we first treated cardiomyocytes with EEDQ, an impermeable alkylating agent that irreversibly binds and inactivates surface dopamine and adrenergic receptors [40]. In our hands, EEDQ totally ablated binding of the hydrophobic non-selective βAR ligand [^{125}I]CYP to HEK 293 cells transfected with the β_2AR (Supplemental Figure 4) but a small fraction of binding was preserved in cardiomyocytes suggesting an internal pool of βAR is protected (Figure 5A). Following alkylation, cardiomyocytes were incubated with ISO (Figure 5B). As seen previously in isolated nuclei, ISO produced an increase in 18S rRNA and this increase was not completely blocked by EEDQ. This supports the notion that nuclear βARs are indeed functional in the intact cardiomyocyte independent of the activation status of surface receptors. This notion was further confirmed by measuring levels of Pim-1 mRNA (Figure 5C). Pim-1 is a protein kinase that has been linked to the pro-survival effects of PKB, and has been shown to play a role in apoptosis and transcriptional activation [41, 42]. Pim-1 mRNA was also increased following ISO treatment, and again EEDQ treatment did not completely block this increase. Thus, although ISO is highly hydrophilic, it is able to enter cardiomyocytes. This has already been shown for norepinephrine [43], and it is believed that an active transporter, norepinephrine-uptake-2, is responsible for the uptake of catecholamines into the cardiomyocyte [44]. However, we cannot exclude the possibility that some surface receptors were spared in the treatment with EEDQ and thus we sought another, more direct way to show that internal receptors could be activated in the intact cell context.

To selectively target the nuclear receptors, we used caged agonists for both ETRs (caged ET-1; cET-1, [29]) and βARs (caged isoproterenol; ZCS-1-67). The “cages” are protecting groups that allow these compounds to freely cross the plasma membrane but can be removed by exposure to UV light, resulting in release of the parent compound with no residual structural modification (e.g., ET-1 or ISO). To first test the caged βAR ligand, we performed direct uncaging experiments in solution by exposing the compounds to UV light before incubating them with HEK 293 cells transfected with the β_2AR. As can be seen in Figures 6A and 6B, at concentrations as high as 10 μM, the caged ISO analog, ZCS-1-67, was not able to significantly

activate βAR signaling until uncaged by exposure to UV light, as measured by stimulation of cAMP production in an EPAC-based BRET assay. Caged ET-1 has been characterized previously [29]. Similarily, radioligand binding assays in membranes prepared from whole rat heart revealed that at concentrations of 1 and 5 μM, caged ZCS-01-67 produced a non-significant reduction in [^{125}I]CYP binding (Figure 6C). Upon photolysis of 1 μM ZCS-01-67, no further reduction was observed, whereas photolysis of 5 μM ZCS-01-67 reduced [^{125}I]CYP binding to a similar extent to that observed with 1 μM ISO. These data indicate that, like alprenolol (a non-selective βAR antagonist) and ISO (a non-selective βAR agonist) uncaged ZCS-01-67 competes with [^{125}I]CYP for binding to βAR. Caged ZCS-01-67 may also compete with [^{125}I]CYP, but very weakly in comparison with ISO, alprenolol, or uncaged ZCS-01-67. Taken together, these data indicate that, at best, ZCS-01-67 may act as a very weak partial agonist (which may still compete for binding to surface receptors) for βARs, having both reduced affinity and efficacy.

We next investigated whether we could still detect increases in NO production following ISO treatment in the intact cardiomyocyte. Measurements of intracellular NO release were performed using live-cell confocal fluorescence microscopy. Cardiomyocytes were loaded with either cET-1 or ZCS-1-67. Higher concentrations of the caged ligands were used to compensate for the reduced UV intensity used to uncage them (to preserve cell viability). Once loaded with agonist, cardiomyocytes were washed to remove excess ligand, and subsequently exposed to a 4 s pulse of UV light (405 nm/30 mW diode, 100% laser intensity) in order to photolyse the caged ligands. Cardiomyocytes were also loaded with a cell-permeable analog of DAF-2, DAF-2 DA, which is hydrolysed to DAF-2 by intracellular esterases, and the fluorescent DNA dye, DRAQ5. Changes in intracellular NO were assessed by monitoring DAF-2 fluorescence using a Zeiss LSM 710 DUO confocal microscope: DRAQ5 fluorescence was measured to delineate the nucleus and quantify changes in nuclear DAF-2 fluorescence (Figure 7A). DAF-2 and DRAQ5 fluorescence was acquired simultaneously. Both cET-1 and ZCS-1-67 evoked increases in NO upon photolysis and this increase was blocked by pre-treatment with L-NAME (Figure 7B). Including ETA (BQ610, 1 μM) and ETB (BQ788, 1 μM) antagonists in the extracellular medium

did not prevent the effects of cET-1, indicating that photolysed ET-1 was not being secreted by the cells and acting upon ETRs at the cell surface (CM and BGA, manuscript in preparation), These results reinforce our findings using EEDQ and support the conclusion that nuclear ETB and β_3AR regulate NO production locally in the nucleus, independently of cell surface receptors. The whole cell images reveal that 5 min after photolysis, the increase in DAF-2 fluorescence induced by cET-1 and ZCS-1-67 differed in terms of compartmentalization. cET-1 increased DAF-2 fluorescence within the nucleus to a level similar to that in the surrounding cytosol (Figure 7C, panel 2). This increase was not observed in the vehicle control (also exposed to UV) or in the presence of cET-1 plus L-NAME (Figure 7C, panels 1 and 3, respectively). In contrast, although ZCS-1-67 produced a significant increase in nuclear NO levels (Figure 7A,B), its effects were far more pronounced in extra-nuclear compartments (Figure 7C, panel 4). In addition, ZCS-1-67 induced a greater overall increase in whole-cell DAF-2 fluorescence than observed with cET-1 (data not shown). The increase in DAF-2 fluorescence induced by ZCS-1-67 was also inhibited by L-NAME (Figure 7C, bottom panel).

4. Discussion

We have demonstrated that the ETB and βAR in the nuclear membrane regulate NO production in isolated cardiac nuclei and more importantly, in intact cardiomyocytes. Using a NO-sensitive fluorescent dye, DAF-2, we observed an increase in NO production following treatment with both ISO and ET-1. In addition, pre-treatment with the NOS inhibitor L-NAME blocked the increase in DAF 2 fluorescence, clearly indicating that these two agonists enhance NOS activity in the nucleus. These results implicate NO in the regulatory effects mediated by these two nuclear GPCRs, including calcium handling for the ETRs and regulation of gene expression for the βARs [7, 45].

Nuclear lysophosphatidic acid receptors (LPAR) have been shown to upregulate iNOS expression in porcine cerebral microvascular endothelial cells through the activation of the PI3K/PKB pathway, and in a PTX-sensitive manner [34]. Moreover, in isolated hepatocyte nuclei, this upregulation is dependent on nuclear eNOS activation [20]. Furthermore the nuclear prostaglandin E_2 receptor (EP_3) has been shown to lead to an increase in both iNOS and eNOS expression in microvessel endothelial cells, through the activation of the ERK1/2 pathway, also in a PTX-sensitive manner [19, 33]. In addition, the nuclear bradykinin B2 receptors (B2Rs) also appear to regulate iNOS expression in isolated hepatocyte nuclei, again through the PI3K/PKB pathway [18]. This is the first study examining the effects of nuclear GPCRs on the NO pathway in adult cardiomyocytes and exact NOS subtype(s) being activated remains to be determined. However, since iNOS expression is not detected in isolated adult cardiac myocytes and iNOS mRNA is only detected after 6 h of stimulation with cytokines [46], it is unlikely that iNOS is responsible for the NO release induced by ISO or ET-1 in isolated cardiac nuclei (30 min) or cardiomyocytes (5 min). In contrast, both eNOS and nNOS are constitutively expressed in heart and appear to have overlapping subcellular distribution and function [47]. In general, eNOS is more abundant at the sarcolemma whereas nNOS is more predominant at the sarcoplasmic reticulum. However, in response to external stimuli nNOS may relocate to the cell periphery

whereas eNOS shifts to intracellular sites, including the nucleus (see [11]). In contrast, in HUVECs, eNOS localizes to the perinuclear region, cytosol, and cell periphery but then translocates to the cell periphery during hypoxia [48]. Although we demonstrated the presence of eNOS immunoreactivity in isolated cardiac nuclei, further study is required to determine the identity and localization of the NOS subtypes activate by ET-1 and isoproterenol in cardiac nuclear membranes.

Given the presence of both β_1AR and β_3AR in cardiac nuclear membranes [4], as well as the propensity of these receptors to interact with multiple G proteins [38, 49], we also investigated which receptor and G protein subtypes were specifically involved in regulating NOS activity. We established that β_3AR was likely responsible for the observed increase in NO production, as the β_3AR selective agonist, BRL 37344, reproduced the stimulatory effect seen with ISO, whereas the β_1AR selective agonist, xamoterol, had no effect. In addition, treatment with forskolin, which directly activates adenylyl cyclase (AC), was also without effect. Taken together, and given the already established link between the nuclear β_1AR and AC/cAMP activation [4], it would appear that the β_1AR-AC/cAMP pathway does not regulate NO production at the level of the nucleus, while the β_3AR does. This is not entirely surprising as it has already been demonstrated that the β_3AR can activate all three NOS subtypes in the heart, and appears to be an important mediator of NO signaling [10]. We also demonstrated that Gαi played a role in this regulation, as its inhibition with PTX resulted in an increase in NO production. Further treatment with either agonist did not potentiate this effect. The mechanism by which Gαi inhibits NO production under basal conditions remains unclear, although the relationship between Gαi and NOS regulation is well established [50, 51], including in regards to nuclear GPCRs [33, 34]. While the nuclear β_3AR has already been shown to signal through $G\alpha_i$ [4], no such link has yet been established for the nuclear ETB. While the β_3AR is only expressed at low levels in cardiomyocytes under basal conditions, its expression does increase during the development of hypertrophy and heart failure [52]. As such, the pathways activated by nuclear β_3AR might play a role in the development of cardiac pathology. Moreover, given the lack of the

β_2AR subtype at the level of the nucleus, the β_3AR may represent a greater proportion of the nuclear βARs as compared to total heart βAR density.

We have also demonstrated that the PI3K/PKB signaling pathway is involved in the regulation of NO production by the βARs, as treatment with the PKB inhibitor triciribine potentiated the effect of ISO. Triciribine however had no effect on basal NO production. The PI3K/PKB pathway is a known regulator of NO production [17, 21, 50, 53], and has been previously linked to nuclear βAR activation [7], and to the upregulation of iNOS expression [18, 34]. The fact that PKB inhibition potentiated the effect of ISO indicates that multiple pathways might be activated following ISO treatment, with both stimulatory and inhibitory pathways being activated. The ability of NO to attenuate signaling of serine/threonine protein kinases may also play a factor in this complex cascade [22]. The possibility of differential effects depending on the NOS subtype being targeted also merits consideration.

We have now demonstrated that NO is involved in the previously characterized regulation of global transcription by nuclear βARs. When examining *de novo* gene transcription in isolated nuclei, we noted that treatment with the NOS inhibitor L-NAME decreased the basal level of *de novo* gene transcription, while also blocking the observed increase following ISO treatment. No appreciable effect was seen in the ET-1 treated samples, indicating that NO signaling is differentially compartmentalized for the two receptor subtypes (as shown in Figure 7C). This likely indicates that NO is indeed involved to some degree in βAR-mediated regulation of gene transcription. This isn't all that surprising given the pre-established role of NO in the regulation of gene transcription through modulation of nuclear NF-κB[16], and that the nuclear β_3AR also appears to regulate the NF-κB pathway [7]. Moreover, we have also shown that PKG is involved in this pathway as well. Similarly to the treatment with L-NAME, treatment with KT5823 or Rp-8-R, potent and selective PKG inhibitors, reduced the basal level of *de novo* gene transcription, and was also able to block the observed increase following ISO treatment. That PKG is a well-established downstream mediator of NO, and has also been shown to regulate PKB and calcium signaling [9], only reinforces these findings.

We also wanted to show that the regulation of NO production observed in isolated nuclei could be observed in the intact cardiomyocyte. Toward this end, we have first shown that nuclear βARs in isolated cardiomyocytes can in fact respond to extracellular ISO, as cells pre-treated with EEDQ, a potent irreversible alkylating agent [40], to inactivate cell surface receptors, still showed an increase in 18S rRNA by qPCR following ISO treatment, as previously observed in isolated nuclei [7]. An increase in levels of Pim-1 mRNA, a protein kinase downstream of PKB [41], was also observed, indicating that mRNA is also regulated by nuclear βARs in intact myocytes. These results do not discount the possibility that nuclear βARs are directly trafficked to the nucleus following their biosynthesis, and not after internalization, as internalized receptors would still have EEDQ bound and thus would remain unable to respond to agonist treatment. The recent identification of nuclear localization sequences in the α_1ARs [54], reveals the need for further study of the βAR in this regard.

Finally, we showed that both the βARs and ETRs can in fact regulate NO production in the intact cardiomyocyte, as treatment with a caged ISO analog (ZCS-1-67) as well as with caged ET-1 (cET-1) resulted in increased NO production as visualized by an increase in DAF-2 fluorescence by live cell confocal microscopy. These caged compounds can freely enter cardiomyocytes allowing us to specifically target intracellular receptors and demonstrate conclusively that internal receptors are functional in the intact cardiomyocyte. These results are further supported by the fact that pre-treatment with L-NAME was able to block this observed increase. These results confirm our previous findings in regard to NO regulation and lend further credence to the notion that nuclear GPCRs do in fact play a role *in vivo*.

5. Conclusions

We have shown that the nuclear β_3AR and ETB regulate NO production in the cardiomyocyte, and that Gαi is implicated in this regulation. Increased NO production was required for the ISO-mediated increase in *de novo* transcription. Furthermore, both PKB and PKG are involved in this pathway. Moreover, we have demonstrated that nuclear receptors can regulate both rRNA and mRNA targets even in the context of the intact cell. Taken together, these results demonstrate for the first time that nuclear GPCRs directly upregulate NO production, and imply that the NO-GC-PKG pathway is involved in the regulation of gene transcription by nuclear GPCRs, as well as that this pathway is active in cardiomyocytes. Furthermore, the spectrum of effects of βAR ligands may be strongly influenced both by their receptor subtype selectivity and their ability to cross the plasma membrane and modulate signaling in βARs located on the nuclear membranes.

Acknowledgements

This work was supported by grants from the Canadian Institutes of Health Research (MOP-77791 to BGA and MOP-79354 and MOP-119530 to TEH), the Fondation des Maladies du Coeur du Québec (to BA) the Fonds de l'Institut de Cardiologie de Montréal (FICM). BGA was a New Investigator of the Heart and Stroke Foundation of Canada and a Senior Scholar of the Fonds de la Recherche en Santé du Québec (FRSQ). TEH holds a Chercheur National award from the FRSQ. SN holds the Paul-David Chair in Cardiovascular Electrophysiology. CM is the recipient of a fellowship from the Heart and Stroke Foundation of Canada. AT is recipient of FRSQ-RSCV/HSFQ doctoral scholarship. IG was supported by a scholarship from the McGill CIHR Drug Development Training Program. We thank Dr. Nicolas Audet, McGill University for critical comments on the manuscript.

Abbreviations

*The abbreviations used are: βAR, β-adrenergic receptor; αAR, α-adrenergic receptor; cET-1, caged ET-1; ISO, isoproterenol; ET-1, endothelin 1; ETB, endothelin type B receptor; ETR, endothelin receptor; GC, guanylyl cyclase; GPCR, G protein-coupled receptor; NO, nitric oxide; NOS nitric oxide synthase; PI3K, phosphoinositide 3-kinase; PKB, protein kinase B; PKG, protein kinase G; cGMP, cyclic guanosine 3',5'-monophosphate; AC, adenylyl cyclase; NFκB, nuclear factor kappa-light-chain-enhancer of activated B-cells; PTX, pertussis toxin; DAF-2, diaminofluorescein-2; PMSF, phenylmethanesulphonylfluoride; DTT, dithiothreitol; EEDQ, *N*-ethoxycarbonyl-2-ethoxy-1,2-dihydroquinoline; PBS, phosphate buffered saline; TCA, trichloroacetic acid; ATP, adenosine triphosphate; UTP, uridine 5' triphosphate; DNA, deoxyribonucleic acid; RNA, ribonucleic acid; qPCR, quantitative real-time polymerase chain reaction; TX-100, Triton X-100.

Figure legends

Figure 1: Synthesis of a caged isoproterenol analog. N-(2-nitrobenzyl)-L-isoproterenol (ZCS-1-67) was synthesized as described in *Methods*.

Figure 2: Effect of various agonists on NO production. Enriched nuclear fractions were preincubated with the fluorescent dye DAF-2 (5 μg/mL), then stimulated with either A) 1 μM isoproterenol or 100 nM ET-1, in the absence or presence of the NOS inhibitor L-NAME (1 mM). B) NO production in response to 1 μM isoproterenol, 100 nM forskolin, 1 μM xamoterol, or 1 μM BRL 37344. C) NO production in response to 1 μM isoproterenol in the presence or absence of 5 nM CGP20712, 10 nM ICI 118,551 or 1 μM SR59230A. NO production was determined as a measure of DAF-2 fluorescence at wavelengths of 485 nm (excitation) and 510 nm (emission). Data represents mean ± S.E. of at least three separate experiments performed in duplicate and are normalized to control. Significant differences (*, $p<0.05$) were determined by one-way ANOVA for three or more experiments.

Figure 3: Effect of pertussis toxin and triciribine on NO production. Enriched nuclear fractions were preincubated with the fluorescent dye DAF-2 (5 μg/mL) and then incubated with either A) the Gαi inhibitor pertussis toxin (PTX, 5 μg/mL), or B) the PKB inhibitor triciribine (1 μM) and then stimulated with 1 μM isoproterenol or 100 nM ET-1. NO production was determined as a measure of DAF-2 fluorescence at wavelengths of 485 nm (excitation) and 510 nm (emission). Data represents mean ± S.E. of at least three separate experiments performed in duplicate and are normalized to control. Significant differences (*, $p<0.05$) were determined by one-way ANOVA for three or more experiments.

Figure 4: Effect of NOS pathway inhibition on isoproterenol and ET-1 induced transcription initiation. A) Enriched nuclear fractions were stimulated with either 1 μM isoproterenol or 100 nM ET-1. [α^{32}P]UTP incorporation was measured in nuclei pre-treated with either vehicle alone (DMSO) or an inhibitor of NOS, L-NAME (1 mM). B) Enriched nuclear fractions were stimulated with either 1 μM isoproterenol, 100 nM ET-1 or 100 μM cGMP. [α^{32}P]-UTP incorporation was measured in nuclei pre-treated with either vehicle alone or inhibitors of PKG, KT5823 (1 μM) or Rp-8-Br (1 μM). C) Enriched nuclear fractions were stimulated with either 100 nM ET-1 or vehicle. RNA was extracted, cDNA prepared, and 18S rRNA quantified by qPCR. C_T values for 18S rRNA were normalized to those for β-actin mRNA. Data represents mean ± S.E. of at least three separate experiments performed in triplicate and are normalized to control. Significant differences (*, $p<0.05$) were determined by one-way ANOVA for three or more experiments.

Figure 5: βARs regulate rRNA and mRNA transcription in intact cardiomyocytes. A) Membranes prepared from freshly isolated myocytes that were preincubated with 100 μM EEDQ or vehicle for 2 h at 37 °C and then lysed. [^{125}I]-CYP (50 μL, 400,000 cpm) was added to 10 μL of membranes in a total volume of 0.5 mL, in triplicate, for each condition. Alprenolol (10 μM) was used to measure non-specific binding. Membranes were incubated at room temperature for 90 min and subsequently captured and washed using a Brandel cell harvester. [^{125}I]-CYP binding was quantified using a γ-counter. B) Enriched nuclear fractions were preincubated with 100 μM EEDQ or vehicle, then stimulated with either 1 μM isoproterenol. RNA was extracted, cDNA prepared and 18S rRNA quantified by qPCR. C_T values for 18S rRNA were normalized to those for β-actin mRNA. C) Enriched nuclear fractions were preincubated with 100 μM EEDQ or vehicle, then stimulated with either 1 μM isoproterenol. RNA was extracted, cDNA prepared and Pim-1 mRNA quantified by qPCR. C_T values for Pim-1 mRNA were normalized to those for β-actin mRNA. Data represents mean ± S.E. of at least three separate experiments. Significant differences (*, $p<0.05$) were determined by one-way ANOVA for three or more experiments.

Figure 6: Activation of βAR signaling by a caged isoproterenol analog, ZCS-1-67, in HEK 293 cells. A) To assess cAMP/PKA pathway activation of endogenous β-adrenergic receptors, an EPAC assay was used. HEK 293 cells were transfected with 1.5 μg of EPAC, a cAMP-sensitive BRET-based biosensor. 48 h later, real-time BRET ratios were measured with 10 μM isoproterenol, vehicle or caged/uncaged ZCS-1-67. The caged compounds were exposed to 15 min of UV light (black-ray long wave, model B100AP lamp) 3.0 cm above the plate to uncage compounds prior to the assay. To calculate net BRET, variations in BRET ratio (ΔBRET) were calculated for each treatment and subtracted from ΔBRET associated to vehicle treated cells. Average of net BRET values representative of three independent experiments. B) Dose-responses for isoproterenol, caged and un-caged isoproterenol analog, ZCS-1-67, were assessed by EPAC assay. The assay was performed as described above and average net BRET responses of three independent experiments were calculated for various concentrations of the compounds. C) βAR ligand binding in membranes prepared from adult rat hearts. [^{125}I]CYP (50 μL, 400,000 cpm) was added to 10 μL of membranes in a total volume of 0.5 mL, 5 replicates were used for each condition. Alprenolol (10 μM), ISO (1 μM), caged or uncaged ZCS-1-67 (1 and 5 μM) were used to compete with specific CYP binding. Membranes were incubated at room temperature for 90 min and subsequently filtered and washed using a Brandel Cell h\Harvester. [^{125}I]CYP binding was quantified using a γ-counter. Data represents mean ± S.E. of at least three separate experiments. Significant differences (*, $p<0.05$) were determined by one-way ANOVA for three or more experiments.

Figure 7: Measurement of NO production in live cardiomyocytes by confocal microscopy. A) Ventricular cardiomyocytes were isolated from adult male rats, allowed to rest for 1 h, then loaded with DAF-2 DA (5 μg/mL) and DRAQ5. Cardiomyocytes were then treated with either ZCS-1-67 (30 μM), cET-1 (1.5 μM), a caged analog of ET-1 or vehicle, as described in *Methods*. Ligand photolysis and fluorescence imaging were accomplished using a Zeiss LSM 7 Duo microscope. Nucleoplasmic DAF-2 fluorescence was recorded before (F_0), during, and after

photolysis (F). DRAQ5 fluorescence was used to delineate the nucleus. Representative traces are shown. B) Nucleoplasmic DAF-2 fluorescence before (F_0) and after (t=500 s: F) photolysis. Signals are presented as background-subtracted normalized fluorescence ($\%F/F_0$), where F is the fluorescence intensity and F_0 is the basal level of DAF-2 fluorescence recorded 1 s prior to photolysis. Data represents mean ± S.E. of at least three separate experiments. Significant differences (*, $p<0.05$) were determined by one-way ANOVA. C) Images showing whole cell DAF-2 and DRAQ5 fluorescence acquired immediately before photolysis (time = 0 s) and 5 min after photolysis of cET-1 or ZCS1-67. Arrows indicate the position of the nuclei in each cell.

Supplemental Figure Legends

Supplemental Figure 1: Regulation of NO production.

Enriched nuclear fractions were preincubated with the fluorescent dye DAF-2 (5 μg/ml), then stimulated with either 1 μM isoproterenol or 100 nM ET-1 for either 5, 10, 15 or 30 min. NO production was determined as a measure of DAF-2 fluorescence at wavelengths of 485 nm (excitation) and 510 nm (emission). Data represents mean ± S.E. of at least three separate experiments performed in duplicate and are normalized to control. Significant differences (*, $p<0.05$) were determined by one-way ANOVA for three or more experiments.

Supplemental Figure 2: Identification of NOS isoforms in isolated nuclei.

A) Bovine aortic endothelial cell lysates (EC; lane 1; 5 μg) and enriched nuclear fractions from three separate preparations (nuclei; lanes 2-4; 100 μg) were separated by SDS-PAGE, transferred to nitrocellulose, and probed with an eNOS-specific antibody. B) Rat brain cytosol (RB; lane 1; 100 μg) and enriched nuclear fractions from three separate preparations (nuclei; lanes 2-4; 100 μg) were separated by SDS-PAGE, transferred to nitrocellulose, and probed with an nNOS-

specific antibody. Membranes were stripped and reprobed using a nucleoporin62-specific antibody (Nup62). The immunoblots shown are representative of 3 independent experiments.

Supplemental Figure 3: Effect of KT5823 on NO production.

Enriched nuclear fractions were preincubated with the fluorescent dye DAF-2 (5 μg/ml) and then stimulated with either 1 μM isoproterenol or 100 nM ET-1, as well as the PKG inhibitors KT5823 (1 μM) or Rp-8-Br (1 μM). NO production was determined as a measure of DAF-2 fluorescence at wavelengths of 485 nm (excitation) and 510 nm (emission). Data represents mean ± S.E. of two separate experiments performed in duplicate and are normalized to control. Significant differences (*, $p<0.05$) were determined by one-way ANOVA for three or more experiments.

Supplemental Figure 4: Effect of EEDQ on βAR binding in HEK 293 cells.

Membranes prepared from native HEK 293 cells and from a stable HEK 293 cell line expressing the β_2AR were preincubated with 100 μM EEDQ or vehicle for 2 h at 37 °C and then lysed. [^{125}I]CYP (50 μl, 400000 cpm) was added to 10 μl of membranes in a total volume of 0.5 ml, in triplicate, for each condition. Alprenolol (10 μM) was used to measure non-specific binding. Membranes were incubated at room temperature for 90 min and subsequently captured and washed using a Brandel cell harvester. [^{125}I]-CYP binding was quantified using a γ-counter.

Disclosure:

The authors declare no conflicts of interest.

References

[1] Tadevosyan A, Vaniotis G, Allen BG, Hebert TE, Nattel S. G protein-coupled receptor signaling in the cardiac nuclear membrane: evidence and possible roles in physiological and pathophysiological function. J Physiol. 2012;590:1313-30.

[2] Vaniotis G, Allen BG, Hébert TE. Nuclear GPCRs in cardiomyocytes: an insider's view of β-adrenergic receptor signaling. Am J Physiol Heart Circ Physiol. 2011;301:H1754-H64.

[3] Boivin B, Chevalier D, Villeneuve LR, Rousseau E, Allen BG. Functional endothelin receptors are present on nuclei in cardiac ventricular myocytes. J Biol Chem. 2003;278:29153-63.

[4] Boivin B, Lavoie C, Vaniotis G, Baragli A, Villeneuve LR, Ethier N, et al. Functional β-adrenergic receptor signaling on nuclear membranes in adult rat and mouse ventricular cardiomyocytes. Cardiovasc Res. 2006;71:69-78.

[5] Sastri M, Barraclough DM, Carmichael PT, Taylor SS. A-kinase-interacting protein localizes protein kinase A in the nucleus. Proc Natl Acad Sci U S A. 2005;102:349-54.

[6] Willard FS, Crouch MF. Nuclear and cytoskeletal translocation and localization of heterotrimeric G-proteins. Immunol Cell Biol. 2000;78:387-94.

[7] Vaniotis G, Del Duca D, Trieu P, Rohlicek CV, Hebert TE, Allen BG. Nuclear β-adrenergic receptors modulate gene expression in adult rat heart. Cell Signal. 2011;23:89-98.

[8] Loscalzo J, Welch G. Nitric oxide and its role in the cardiovascular system. Prog Cardiovasc Dis. 1995;38:87-104.

[9] Hammond J, Balligand JL. Nitric oxide synthase and cyclic GMP signaling in cardiac myocytes: From contractility to remodeling. J Mol Cell Cardiol. 2012;52:330-40.

[10] Moens AL, Yang R, Watts VL, Barouch LA. Beta 3-adrenoreceptor regulation of nitric oxide in the cardiovascular system. J Mol Cell Cardiol. 2010;48:1088-95.

[11] Zhang YH, Casadei B. Sub-cellular targeting of constitutive NOS in health and disease. J Mol Cell Cardiol. 2012;52:341-50.

[12] Hayashi Y, Nishio M, Naito Y, Yokokura H, Nimura Y, Hidaka H, et al. Regulation of neuronal nitric-oxide synthase by calmodulin kinases. J Biol Chem. 1999;274:20597-602.

[13] Hu J, el-Fakahany EE. Intricate regulation of nitric oxide synthesis in neurons. Cell Signal. 1996;8:185-9.

[14] Martins AR, Zanella CA, Zucchi FC, Dombroski TC, Costa ET, Guethe LM, et al. Immunolocalization of nitric oxide synthase isoforms in human archival and rat tissues, and cultured cells. J Neurosci Methods. 2011;198:16-22.

[15] Siednienko J, Nowak J, Moynagh PN, Gorczyca WA. Nitric oxide affects IL-6 expression in human peripheral blood mononuclear cells involving cGMP-dependent modulation of NF-kappaB activity. Cytokine. 2011;54:282-8.

[16] Dawn B, Bolli R. Role of nitric oxide in myocardial preconditioning. Ann N Y Acad Sci. 2002;962:18-41.

[17] Mao M, Sudhahar V, Ansenberger-Fricano K, Fernandes DC, Tanaka LY, Fukai T, et al. Nitroglycerin drives endothelial nitric oxide synthase activation via the phosphatidylinositol 3-kinase/protein kinase B pathway. Free Radic Biol Med. 2012;52:427-35.

[18] Savard M, Barbaz D, Belanger S, Muller-Esterl W, Bkaily G, D'Orleans-Juste P, et al. Expression of endogenous nuclear bradykinin B2 receptors mediating signaling in immediate early gene activation. J Cell Physiol. 2008;216:234-44.

[19] Gobeil F, Jr., Dumont I, Marrache AM, Vazquez-Tello A, Bernier SG, Abran D, et al. Regulation of eNOS expression in brain endothelial cells by perinuclear EP_3 receptors. Circ Res. 2002;90:682-9.

[20] Gobeil F, Jr., Zhu T, Brault S, Geha A, Vazquez-Tello A, Fortier A, et al. Nitric oxide signaling via nuclearized endothelial nitric-oxide synthase modulates expression of the immediate early genes iNOS and mPGES-1. J Biol Chem. 2006;281:16058-67.

[21] Strijdom H, Friedrich SO, Hattingh S, Chamane N, Lochner A. Hypoxia-induced regulation of nitric oxide synthase in cardiac endothelial cells and myocytes and the role of the PI3-K/PKB pathway. Mol Cell Biochem. 2009;321:23-35.

[22] Kapakos G, Bouallegue A, Daou GB, Srivastava AK. Modulatory Role of Nitric Oxide/cGMP System in Endothelin-1-Induced Signaling Responses in Vascular Smooth Muscle Cells. Curr Cardiol Rev. 2010;6:247-54.

[23] Kanai AJ, Mesaros S, Finkel MS, Oddis CV, Birder LA, Malinski T. Beta-adrenergic regulation of constitutive nitric oxide synthase in cardiac myocytes. Am J Physiol. 1997;273:C1371-7.

[24] Provost C, Choufani F, Avedanian L, Bkaily G, Gobeil F, Jacques D. Nitric oxide and reactive oxygen species in the nucleus revisited. Can J Physiol Pharmacol. 2010;88:296-304.

[25] Muralidharan S, Nerbonne JM. Photolabile "caged" adrenergic receptor agonists and related model compounds. J Photochem Photobiol B. 1995;27:123-37.

[26] Tadevosyan A, Maguy A, Villeneuve LR, Babin J, Bonnefoy A, Allen BG, et al. Nuclear-delimited angiotensin receptor-mediated signaling regulates cardiomyocyte gene expression. The Journal of biological chemistry. 2010;285:22338-49.

[27] Lemire I, Allen BG, Rindt H, Hebert TE. Cardiac-specific overexpression of alpha1BAR regulates betaAR activity via molecular crosstalk. J Mol Cell Cardiol. 1998;30:1827-39.

[28] Boivin B, Allen BG. Regulation of membrane-bound PKC in adult cardiac ventricular myocytes. Cell Signal. 2003;15:217-24.

[29] Bourgault S, Letourneau M, Fournier A. Development of photolabile caged analogs of endothelin-1. Peptides. 2007;28:1074-82.

[30] Masri B, Salahpour A, Didriksen M, Ghisi V, Beaulieu JM, Gainetdinov RR, et al. Antagonism of dopamine D2 receptor/β-arrestin 2 interaction is a common property of clinically effective antipsychotics. Proc Natl Acad Sci U S A. 2008;105:13656-61.

[31] Chevalier D, Allen BG. Two distinct forms of MAPKAP kinase-2 in adult cardiac ventricular myocytes. Biochemistry. 2000;39:6145-56.

[32] Jaureguiberry MS, di Nunzio AS, Dattilo MA, Bianciotti LG, Vatta MS. Endothelin 1 and 3 enhance neuronal nitric oxide synthase activity through ETB receptors involving multiple signaling pathways in the rat anterior hypothalamus. Peptides. 2004;25:1133-8.

[33] Bhattacharya M, Peri K, Ribeiro-da-Silva A, Almazan G, Shichi H, Hou X, et al. Localization of functional prostaglandin E2 receptors EP3 and EP4 in the nuclear envelope. J Biol Chem. 1999;274:15719-24.

[34] Gobeil F, Jr., Bernier SG, Vazquez-Tello A, Brault S, Beauchamp MH, Quiniou C, et al. Modulation of pro-inflammatory gene expression by nuclear lysophosphatidic acid receptor type-1. J Biol Chem. 2003;278:38875-83.

[35] John TA, Ibe BO, Raj JU. Regulation of endothelial nitric oxide synthase: involvement of protein kinase G 1β, serine 116 phosphorylation and lipid structures. Clinical and experimental pharmacology & physiology. 2008;35:148-58.

[36] John TA, Raj JU. A fluorescence-activated cell sorter analysis of the relationship between protein kinase G and endothelial nitric oxide synthase. Anat Rec (Hoboken). 2010;293:1755-65.

[37] Lavoie C, Hebert TE. Pharmacological characterization of putative beta1-beta2-adrenergic receptor heterodimers. Can J Physiol Pharmacol. 2003;81:186-95.

[38] Brunner F, Brás-Silva C, Cerdeira AS, Leite-Moreira AF. Cardiovascular endothelins: essential regulators of cardiovascular homeostasis. Pharmacol Ther. 2006;111:508-31.

[39] Penna C, Rastaldo R, Mancardi D, Cappello S, Pagliaro P, Westerhof N, et al. Effect of endothelins on the cardiovascular system. J Cardiovasc Med (Hagerstown). 2006;7:645-52.

[40] Neve KA, Molinoff PB. Turnover of β_1- and β_2-adrenergic receptors after down-regulation or irreversible blockade. Mol Pharmacol. 1986;30:104-11.

[41] Muraski JA, Fischer KM, Wu W, Cottage CT, Quijada P, Mason M, et al. Pim-1 kinase antagonizes aspects of myocardial hypertrophy and compensation to pathological pressure overload. Proc Natl Acad Sci U S A. 2008;105:13889-94.

[42] Zhang Y, Wang Z, Li X, Magnuson NS. Pim kinase-dependent inhibition of c-Myc degradation. Oncogene. 2008;27:4809-19.

[43] Buu NT, Hui R, Falardeau P. Norepinephrine in neonatal rat ventricular myocytes: association with the cell nucleus and binding to nuclear α_1- and β-adrenergic receptors. J Mol Cell Cardiol. 1993;25:1037-46.

[44] Wright CD, Chen Q, Baye NL, Huang Y, Healy CL, Kasinathan S, et al. Nuclear α1-adrenergic receptors signal activated ERK localization to caveolae in adult cardiac myocytes. Circ Res. 2008;103:992-1000.

[45] Jacques D, Descorbeth M, Abdel-Samad D, Provost C, Perreault C, Jules F. The distribution and density of ET-1 and its receptors are different in human right and left ventricular endocardial endothelial cells. Peptides. 2005;26:1427-35.

[46] Balligand JL, Ungureanu-Longrois D, Simmons WW, Pimental D, Malinski TA, Kapturczak M, et al. Cytokine-inducible nitric oxide synthase (iNOS) expression in cardiac myocytes. Characterization and regulation of iNOS expression and detection of iNOS activity in single cardiac myocytes in vitro. J Biol Chem. 1994;269:27580-8.

[47] Sun J, Morgan M, Shen RF, Steenbergen C, Murphy E. Preconditioning results in S-nitrosylation of proteins involved in regulation of mitochondrial energetics and calcium transport. Circ Res. 2007;101:1155-63.

[48] Prieto CP, Krause BJ, Quezada C, San Martin R, Sobrevia L, Casanello P. Hypoxia-reduced nitric oxide synthase activity is partially explained by higher arginase-2 activity and cellular redistribution in human umbilical vein endothelium. Placenta. 2011;32:932-40.

[49] Zhen MF, Chen JY, Liu F, Dong SM, He YJ, Zhu QK, et al. The operative technique selection of lung transplantation for end-stage emphysema. Zhonghua Wai Ke Za Zhi. 2005;43:1444-6.

[50] Banquet S, Delannoy E, Agouni A, Dessy C, Lacomme S, Hubert F, et al. Role of $G_{i/o}$-Src kinase-PI3K/Akt pathway and caveolin-1 in β-adrenoceptor coupling to endothelial NO synthase in mouse pulmonary artery. Cell Signal. 2011;23:1136-43.

[51] Datar R, Kaesemeyer WH, Chandra S, Fulton DJ, Caldwell RW. Acute activation of eNOS by statins involves scavenger receptor-B1, G protein subunit Gi, phospholipase C and calcium influx. Br J Pharmacol. 2010;160:1765-72.

[52] Zheng M, Zhu W, Han Q, Xiao RP. Emerging concepts and therapeutic implications of beta-adrenergic receptor subtype signaling. Pharmacol Ther. 2005;108:257-68.

[53] Dossumbekova A, Berdyshev EV, Gorshkova I, Shao Z, Li C, Long P, et al. Akt activates NOS3 and separately restores barrier integrity in H2O2-stressed human cardiac microvascular endothelium. Am J Physiol Heart Circ Physiol. 2008;295:H2417-26.

[54] Wright CD, Wu SC, Dahl EF, Sazama AJ, O'Connell TD. Nuclear localization drives α1-adrenergic receptor oligomerization and signaling in cardiac myocytes. Cell Signal. 2012;24:794-802.

Table 1: Primers used for real-time qPCR

Target	Primers
18S Sense	5’- ACG GAC CAG AGC GAA AGC AT -3’
18S Antisense	5’- TGT CAA TCC TGT CCG TGT CC -3’
NFκB Sense	5’- CTG CGA TAC CTT AAT GAC AGC G -3’
NFκB Antisense	5’- AAT TTT GGC TTC CTT TCT TGG CT -3’
β-Actin Sense	5’- TTC AAT TCC ATC ATG AAG TGT G -3’
β-Actin Antisense	5’- CTG ATC CAC ATC TGC TGG AAG GTG -3’

Figure 1

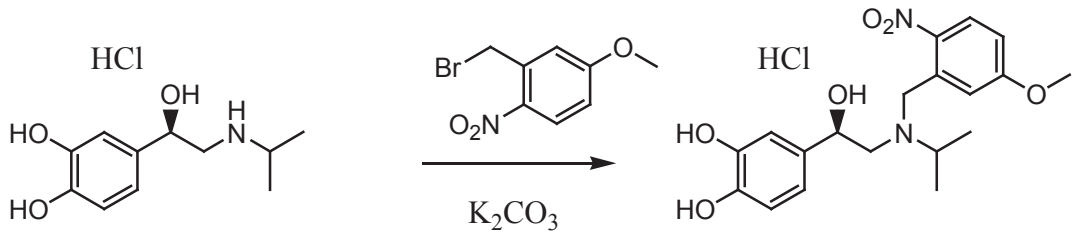

(-)-isoproterenol hydrochloride

Figure 2

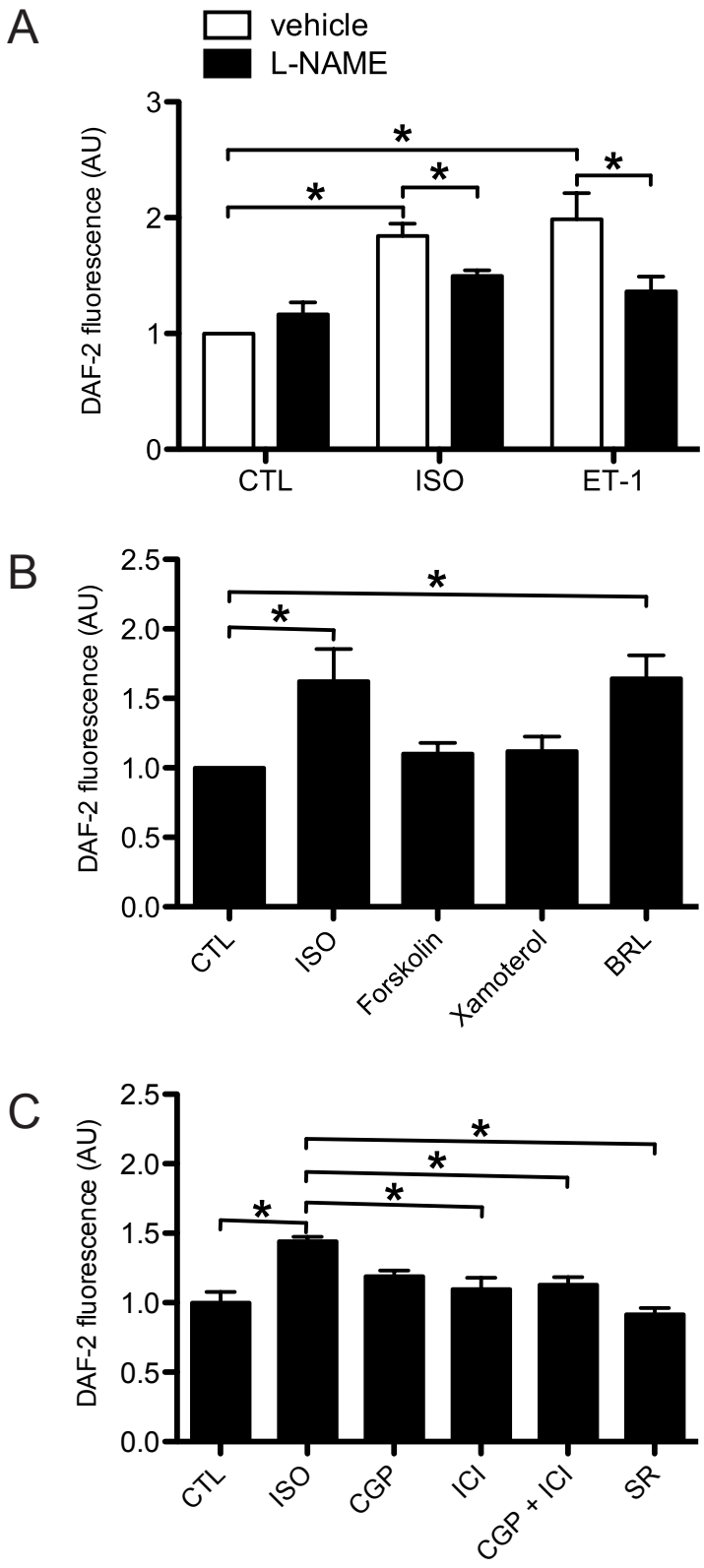
A
vehicle
L-NAME
DAF-2 fluorescence (AU)
3
2
1
0
*
*
*
*
CTL
ISO
ET-1
B
DAF-2 fluorescence (AU)
2.5
2.0
1.5
1.0
0.5
0.0
*
*
CTL
ISO
Forskolin
Xamoterol
BRL
C
DAF-2 fluorescence (AU)
2.5
2.0
1.5
1.0
0.5
0.0
*
*
*
*
CTL
ISO
CGP
ICI
CGP + ICI
SR

Figure 3

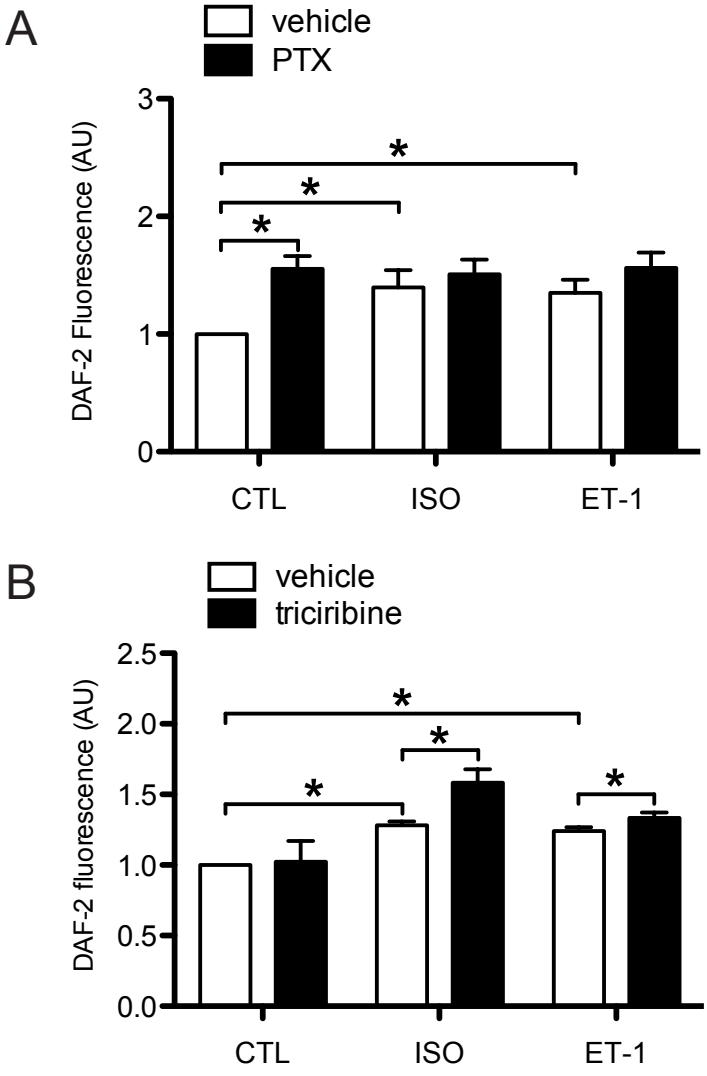
A
vehicle
PTX
DAF-2 Fluorescence (AU)
3
2
1
0
*
*
*
CTL
ISO
ET-1
B
vehicle
triciribine
DAF-2 fluorescence (AU)
2.5
2.0
1.5
1.0
0.5
0.0
*
*
*
CTL
ISO
ET-1

Figure 4

A

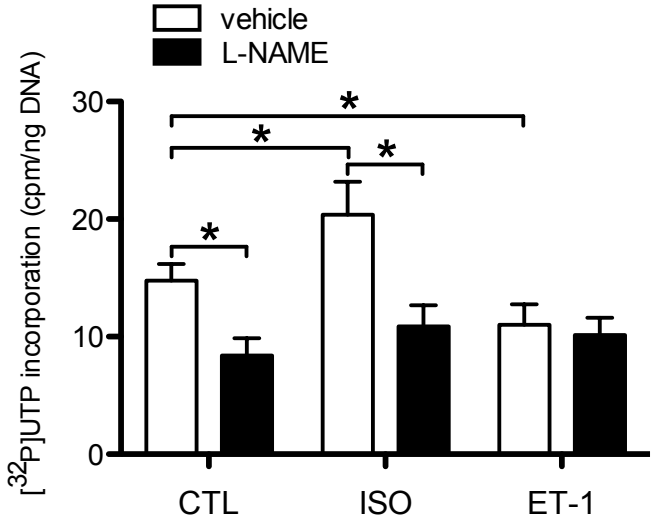
vehicle
L-NAME
[32P]UTP incorporation (cpm/ng DNA)
30
20
10
0
*
*
*
*
CTL
ISO
ET-1

B

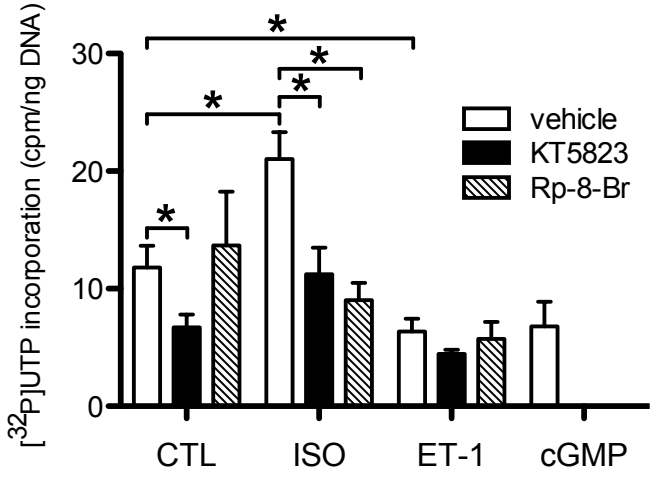
[32P]UTP incorporation (cpm/ng DNA)
30
20
10
0
*
*
*
*
vehicle
KT5823
Rp-8-Br
CTL
ISO
ET-1
cGMP

C

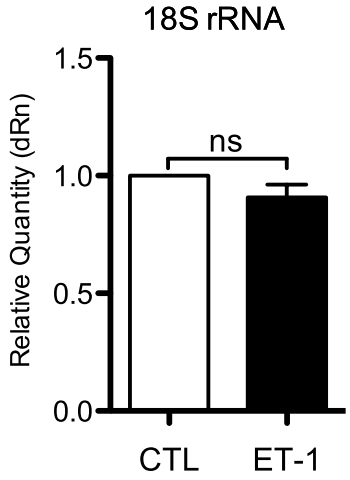
18S rRNA
Relative Quantity (dRn)
1.5
1.0
0.5
0.0
ns
CTL
ET-1

Figure 5

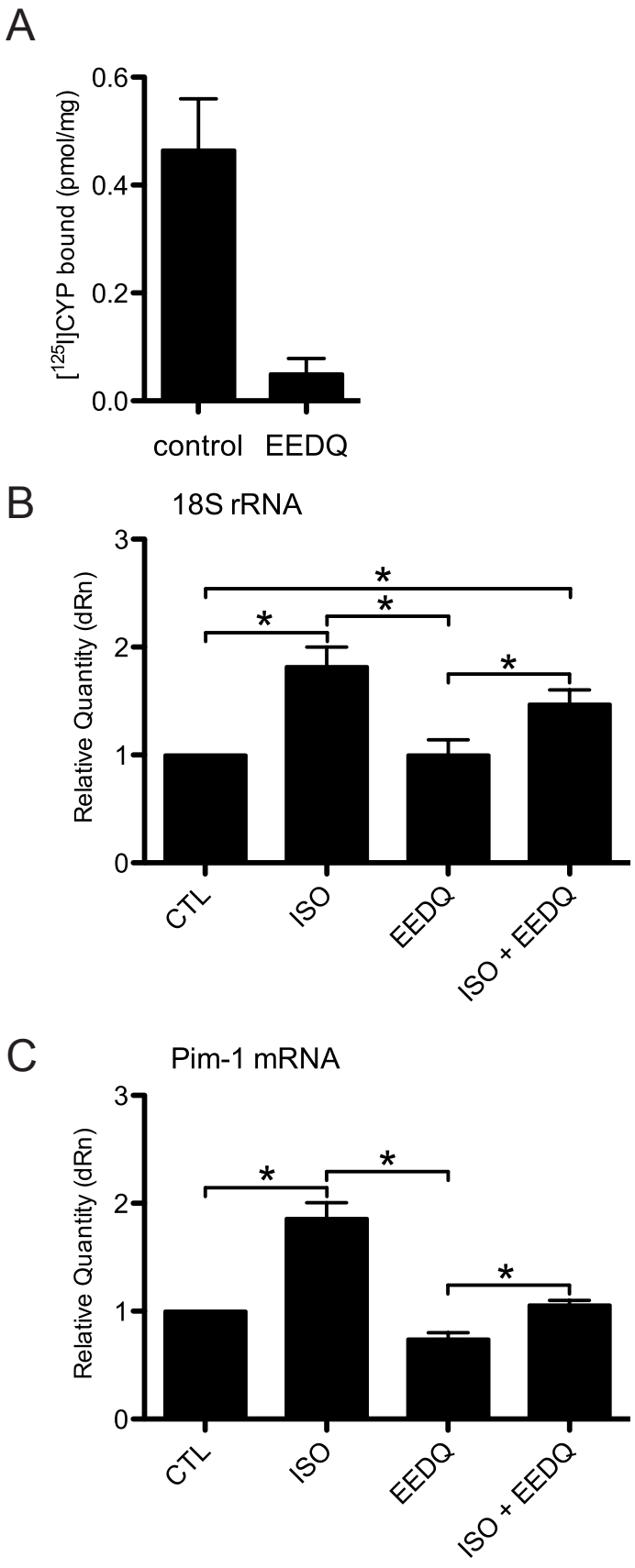
A
0.6
0.4
0.2
0.0
[125]ICYP bound (pmol/mg)
control
EEDQ
B
18S rRNA
Relative Quantity (dRn)
3
2
1
0
*
*
*
*
CTL
ISO
EEDQ
ISO + EEDQ
C
Pim-1 mRNA
Relative Quantity (dRn)
3
2
1
0
*
*
*
CTL
ISO
EEDQ
ISO + EEDQ

Figure 6

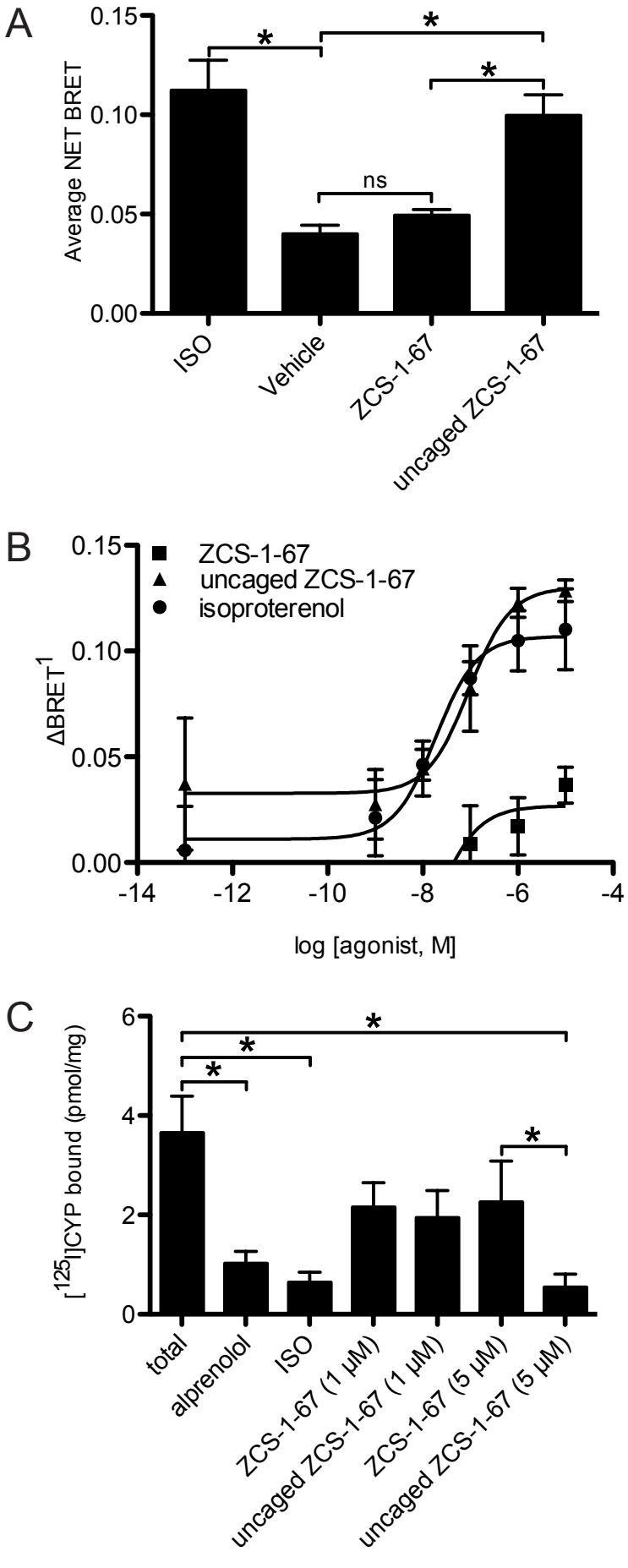
A
Average NET BRET
0.15
0.10
0.05
0.00
*
*
*
ns
ISO
Vehicle
ZCS-1-67
uncaged ZCS-1-67
B
ZCS-1-67
uncaged ZCS-1-67
isoproterenol
ΔBRET-1
0.15
0.10
0.05
0.00
-14
-12
-10
-8
-6
-4
log [agonist, M]
C
[125]CYP bound (pmol/mg)
6
4
2
0
*
*
*
*
total
alprenolol
ISO
ZCS-1-67 (1 μM)
uncaged ZCS-1-67 (1 μM)
ZCS-1-67 (5 μM)
uncaged ZCS-1-67 (5 μM)

Figure 7

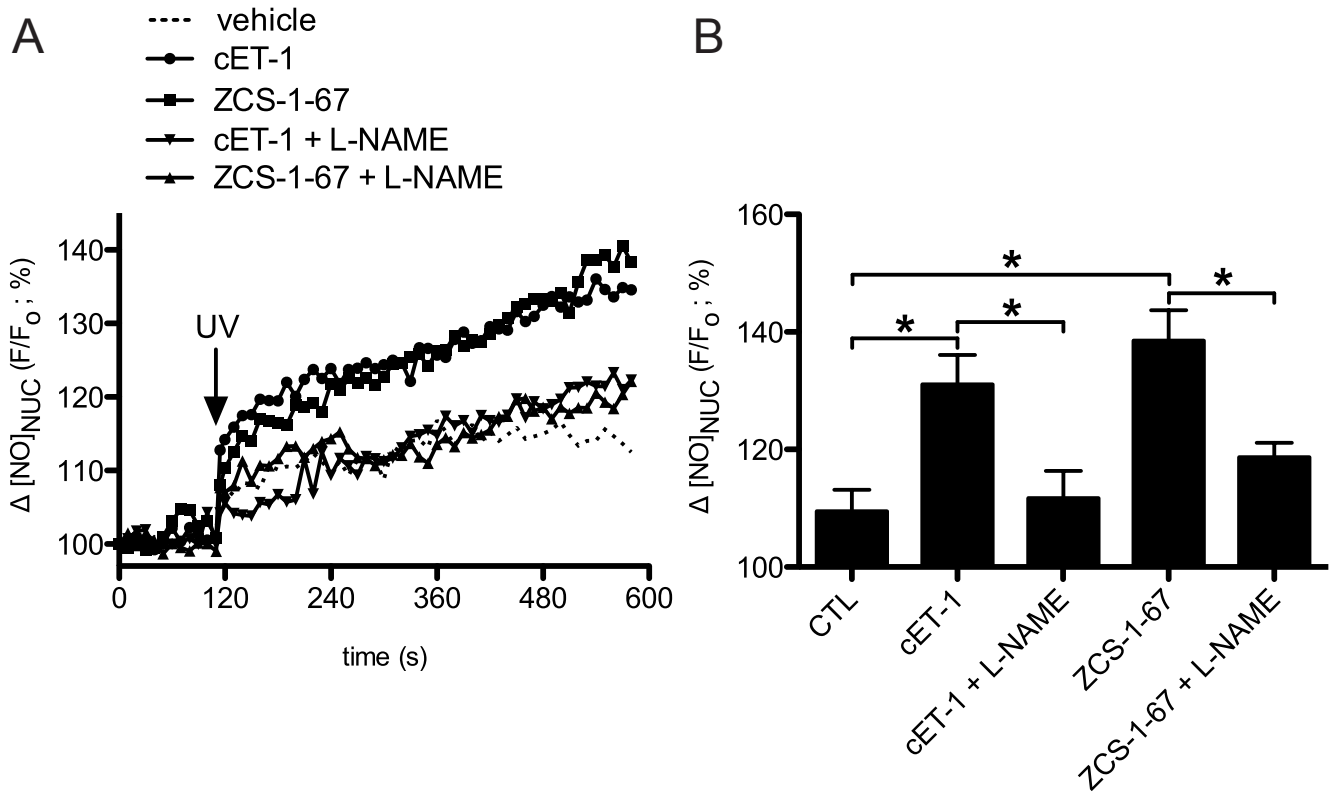
A
vehicle
cET-1
ZCS-1-67
cET-1 + L-NAME
ZCS-1-67 + L-NAME
Δ [NO]NUC (F/FO ; %)
UV
time (s)
B
CTL
cET-1
cET-1 + L-NAME
ZCS-1-67
ZCS-1-67 + L-NAME

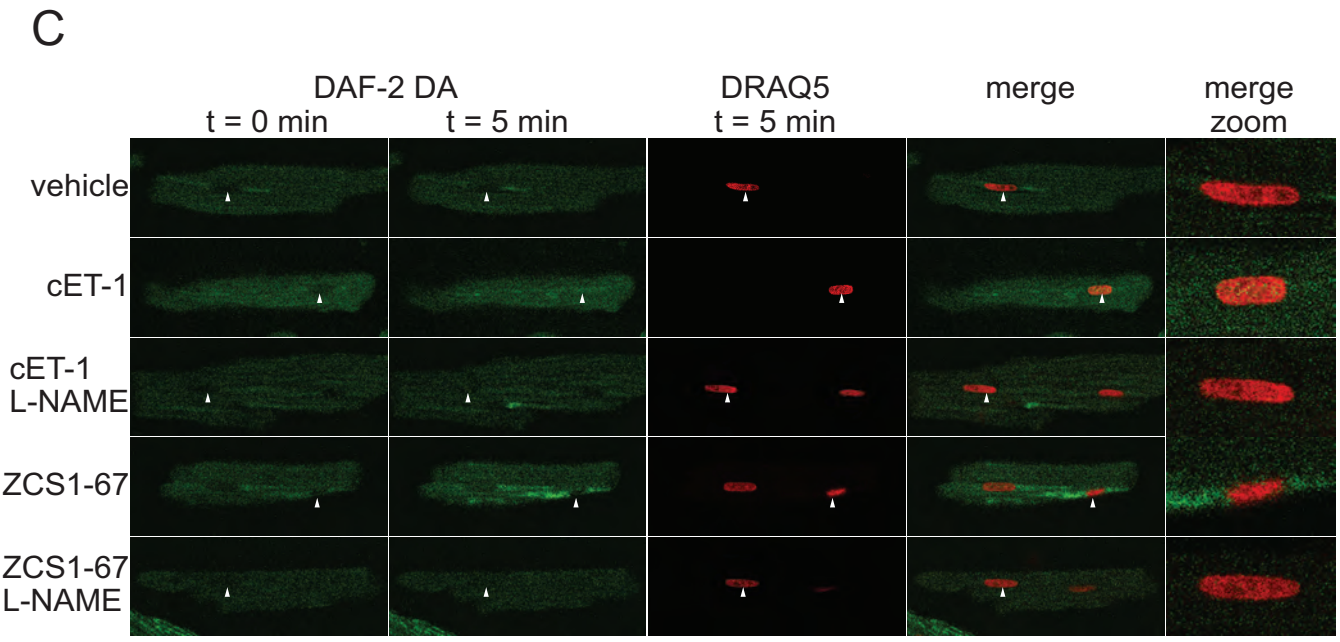
C
DAF-2 DA
t = 0 min
t = 5 min
DRAQ5
t = 5 min
merge
merge
zoom
vehicle
cET-1
cET-1
L-NAME
ZCS1-67
ZCS1-67
L-NAME

Supplemental Figure Legends

Supplemental Figure 1: Regulation of NO production.

Enriched nuclear fractions were preincubated with the fluorescent dye DAF-2 (5 μg/ml), then stimulated with either 1 μM isoproterenol or 100 nM ET-1 for either 5, 10, 15 or 30 min. NO production was determined as a measure of DAF-2 fluorescence at wavelengths of 485 nm (excitation) and 510 nm (emission). Data represents mean ± S.E. of at least three separate experiments performed in duplicate and are normalized to control. Significant differences (*, $p<0.05$) were determined by one-way ANOVA for three or more experiments.

Supplemental Figure 2: Identification of NOS isoforms in isolated nuclei.

A) Bovine aortic endothelial cell lysates (EC; lane 1; 5 μg) and enriched nuclear fractions from three separate preparations (nuclei; lanes 2-4; 100 μg) were separated by SDS-PAGE, transferred to nitrocellulose, and probed with an eNOS-specific antibody. B) Rat brain cytosol (RB; lane 1; 100 μg) and enriched nuclear fractions from three separate preparations (nuclei; lanes 2-4; 100 μg) were separated by SDS-PAGE, transferred to nitrocellulose, and probed with an nNOS-specific antibody. Membranes were stripped and reprobed using a nucleoporin62-specific antibody (Nup62). The immunoblots shown are representative of 3 independent experiments.

Supplemental Figure 3: Effect of KT5823 on NO production.

Enriched nuclear fractions were preincubated with the fluorescent dye DAF-2 (5 μg/ml) and then stimulated with either 1 μM isoproterenol or 100 nM ET-1, as well as the PKG inhibitors KT5823 (1 μM) or Rp-8-Br (1 μM). NO production was determined as a measure of DAF-2 fluorescence at wavelengths of 485 nm (excitation) and 510 nm (emission). Data represents mean ± S.E. of two separate experiments performed in duplicate and are normalized to control. Significant differences (*, $p<0.05$) were determined by one-way ANOVA for three or more experiments.

<u>Supplemental Figure 4</u>: Effect of EEDQ on βAR binding in HEK 293 cells.

Membranes prepared from native HEK 293 cells and from a stable HEK 293 cell line expressing the β_2AR were preincubated with 100 μM EEDQ or vehicle for 2 h at 37 °C and then lysed. [^{125}I]CYP (50 μl, 400000 cpm) was added to 10 μl of membranes in a total volume of 0.5 ml, in triplicate, for each condition. Alprenolol (10 μM) was used to measure non-specific binding. Membranes were incubated at room temperature for 90 min and subsequently captured and washed using a Brandel cell harvester. [^{125}I]-CYP binding was quantified using a γ-counter.

Supplementary Figure 1

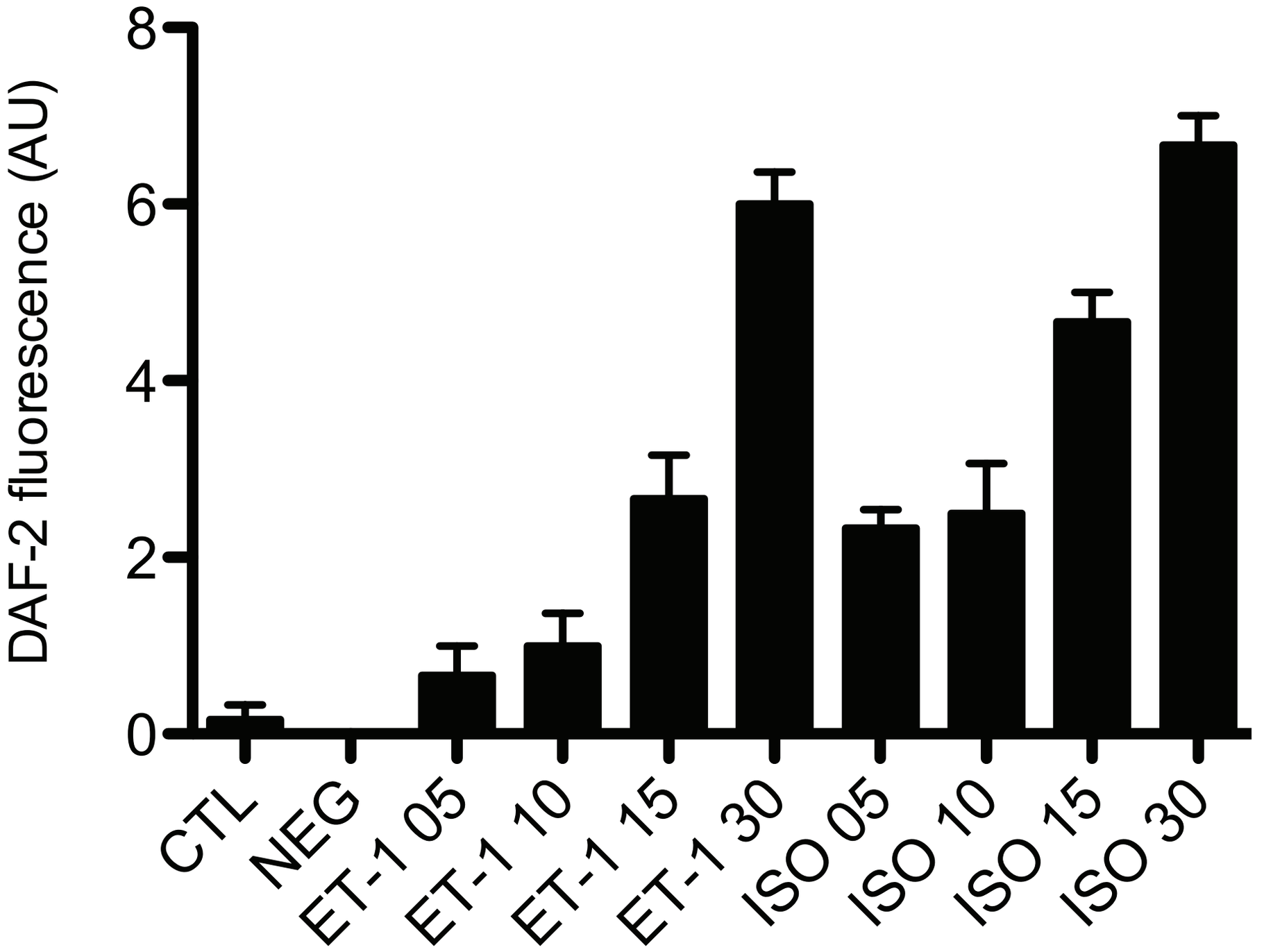

Supplementary Figure 2

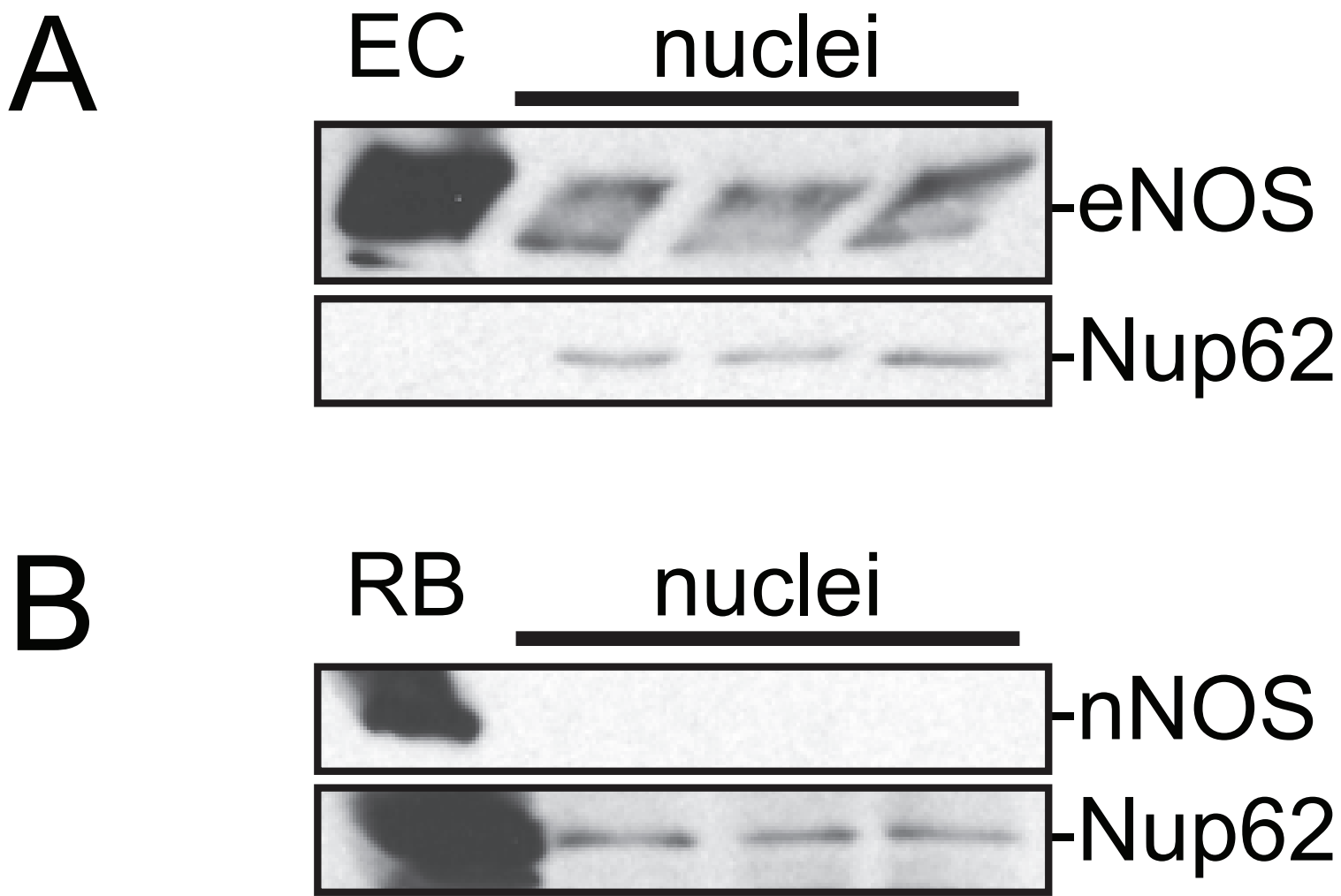

Supplementary Figure 3

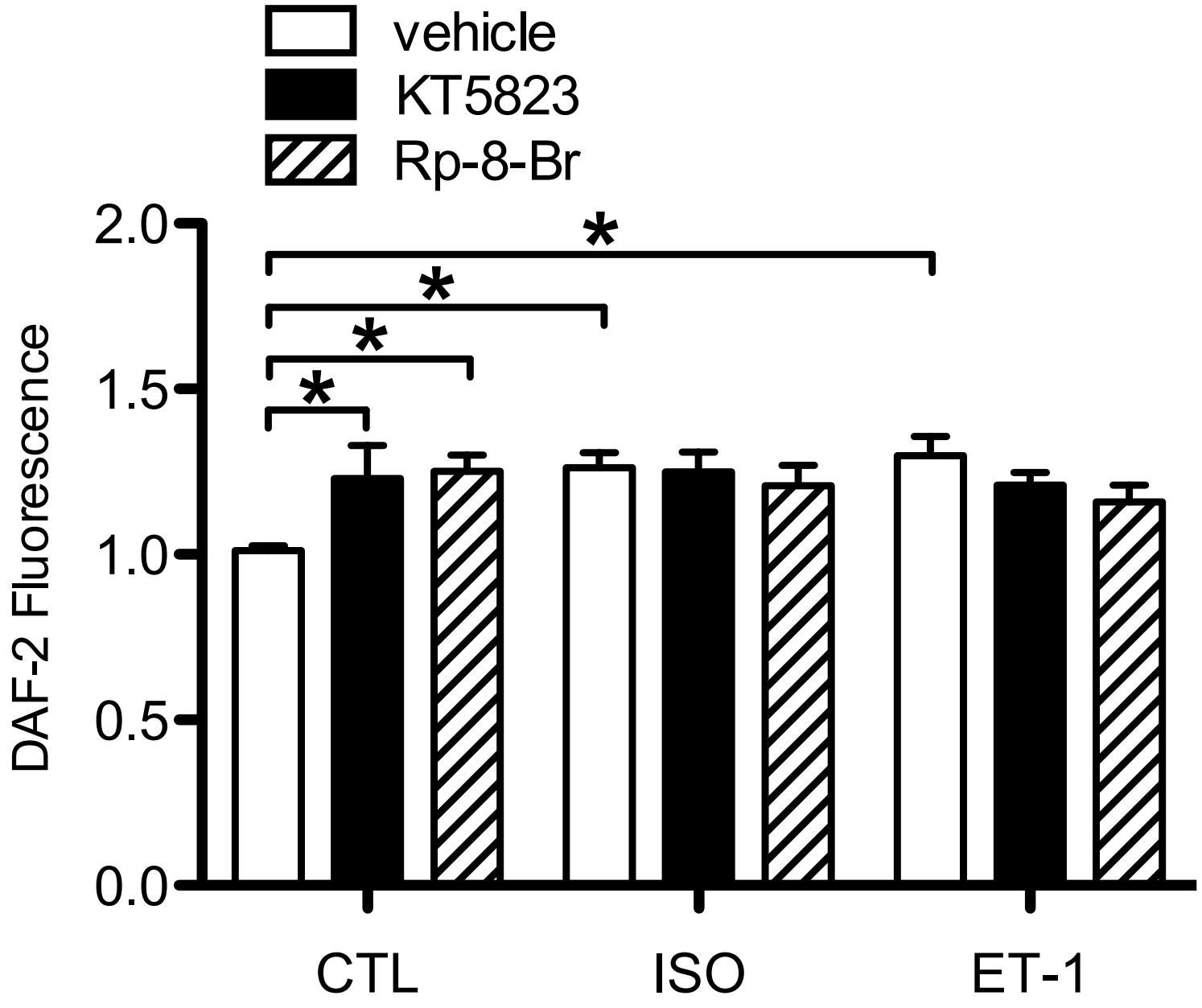

Supplementary Figure 4